Quaternary Geochronology 71 (2022) 101336

Contents lists available at ScienceDirect

Quaternary Geochronology

journal homepage: www.elsevier.com/locate/quageo

Chronology of Early to Mid-Pleistocene sediments in the northern North Sea: New evidence from amino acid and strontium isotope analyses

Teena Chauhan [a,*], Hans Petter Sejrup [a], Berit Oline Hjelstuen [a], Darrell S. Kaufman [b], Irfan Baig [c], Benedict T.I. Reinardy [d]

[a] Department of Earth Science, University of Bergen, Allegaten 41, N-5007, Bergen, Norway
[b] School of Earth and Sustainability, Northern Arizona University, Flagstaff, AZ, 86011, USA
[c] Department of Geosciences, University of Oslo, Blindern, 0316, Oslo, Norway
[d] Department of Physical Geography, Stockholm University and Bolin Centre for Climate Research, Stockholm, 10691, Sweden

ARTICLE INFO

Keywords:
Quaternary
Amino acid racemization
D/L Asp (aspartic acid)
Foraminifera
Elphidium excavatum
$^{87}Sr/^{86}Sr$ values
Sr age
Bruhnes/Matuyama (B/M) boundary
Calibration curve
North Sea geochronology

ABSTRACT

Sediments deposited during glacial-interglacial cycles through the Early to Mid-Pleistocene in the North Sea are chronologically poorly constrained. To contribute to the chronology of these units, amino acid racemization (AAR) and strontium (Sr) isotope analyses have been performed on samples from four shallow borings and one oil well along a transect in the northern North Sea. D/L Asp (aspartic acid) values obtained through reverse-phase liquid chromatography in the benthic foraminiferal species *Elphidium excavatum* is focused on because of consistent results and a good stratigraphic distribution of this benthic species. For the Early Pleistocene, an age model for the well 16/1–8, from the central part of the northern North Sea based on Sr ages allows for dating of the prograding wedges filling the pre-Quaternary central basin. A regional calibration curve for the racemization of Asp in *Elphidium excavatum* is developed using published ages of radiocarbon-dated samples and samples associated with the previously identified Bruhnes/Matuyama (B/M) paleomagnetic boundary and a Sr age from this study. Based on all the available geochronological evidence, samples were assigned to marine oxygen isotope stages (MIS) with uncertainties on the order of 10–70 ka.

Sr ages suggest a hiatus of <2 million years (Ma) possibly due to non-deposition or low sedimentation between the Utsira Formation (Pliocene) and the Early Pleistocene. An increase in sedimentation rates around 1.5 ± 0.07 Ma (~MIS 51) may partly be due to sediment supply from rivers from the south-east and partly due to the extension of ice sheet around 1.36 ± 0.07 Ma from the Norwegian coast to the central North Sea. A possible basin-wide glaciation occurred around 1.1 Ma (~ MIS 32) (upper regional unconformity/top of unit Q4 in this study), resulting in erosion and regional unconformity. Two interglacials in the Norwegian Channel have been dated: the Radøy Interglacial to 1.07 ± 0.01 Ma (possibly MIS 31, the 'super interglacial'), and the Norwegian Trench Interglacial to 0.50 ± 0.02 Ma (possibly MIS 13). A massive till unit identified at the same stratigraphic level in all shallow borings may partly represent an extensive MIS 12 glaciation. This study shows that the combined use of amino acid racemization data and Sr isotope chronology can refine the chronological ambiguities of Quaternary North Sea sediments related partly to the impact of glacial processes.

1. Introduction

Quaternary sediments in the North Sea (Fig. 1) reflect the influence of climate variability, glacial expansions, variability in river drainage, sea-level changes, and tectonic subsidence of the basin. These factors have led to an episodic deposition style and sediment packages up to 1000 m thick (Sejrup et al., 1991, 2000; Lonergan et al., 2006; Ottesen et al., 2018; Hjelstuen and Sejrup, 2020). A key challenge to disentangle the Quaternary depositional history of the North Sea has been to establish robust chronologies in complex glacial-interglacial conditions through the Quaternary including the timing of the first grounded ice in the central North Sea. Earlier chronological studies on the Quaternary

Abbreviations: AAR, amino acid racemization; Asp, aspartic acid; B/M, Bruhnes/Matuyama; Glu, glutamic acid; m, meter, here 'meters below the seafloor'; Ma, million years; MIS, marine oxygen isotope stage; RP-HPLC, reverse-phase high-pressure liquid chromatography; ka, kilo annum; Sr, strontium.

* Corresponding author.
E-mail addresses: Teena.Chauhan@uib.no, chauhan2081@gmail.com (T. Chauhan).

https://doi.org/10.1016/j.quageo.2022.101336
Received 11 July 2021; Received in revised form 4 April 2022; Accepted 6 May 2022
Available online 19 May 2022

sediments of the northern North Sea have been carried out partly on gravity, piston, and vibro cores up to 20 m long (commonly covering the last deglaciation up to present), partly on shallow borings drilled down to maximum *c*. 200 m below the seafloor, and partly on material from hydrocarbon exploration wells at greater depths. The availability of high-quality core material of the Mid and Early Quaternary age has been limited from the North Sea.

Previously, samples from shallow borings from the northern North Sea covering the Mid and Late Pleistocene were dated with methods including radiocarbon, paleomagnetic reversal stratigraphy, strontium (Sr) isotopes, amino acid geochronology, and biostratigraphy (Sejrup et al., 1987, 1989, 1994, 1995; Knudsen and Sejrup, 1993; Sejrup and Knudsen, 1993; Haflidason et al., 1995; Reinardy et al., 2018). The Early Pleistocene sediment package in the North Sea is mostly dated by biostratigraphical methods, and Sr isotopes on cuttings from oil wells (Knudsen and Asbjörnsdóttir, 1991; Eidvin et al., 1999; Eidvin and Rundberg, 2001, 2007; Piasecki et al., 2002; Head et al., 2004; Rea et al., 2018) and only limited amino acid work has been published using reverse-phase liquid chromatography (Reinardy et al., 2017). As each of these dating methods has its limitations, results from different methods are commonly used in combination to improve the accuracy of age estimates.

Amino acid racemization (AAR) is considered a good tool to locate hiatuses and reworking in the Quaternary sedimentary sequences; however, since the reaction rates are highly temperature-dependent, it is challenging to provide numerical dates (Brigham-Grette and Sejrup, 1985; Wehmiller et al., 2012). Except for the work by Reinardy et al. (2017, 2018), which used reverse-phase high-pressure liquid chromatography (RP-HPLC) and presented D/L Ile values (extent of epimerization of L-isoleucine to D-alloisoleucine), other previous North Sea amino acid geochronological studies measured the same reaction using conventional ion-exchange HPLC method, and ratios were presented as A/I values (Sejrup et al., 1987, 1995, 1998; Knudsen and Sejrup, 1988, 1993; Sejrup and Knudsen, 1999).

To establish robust chronology, we have combined AAR analyses based on RP-HPLC, with Sr isotope dating on multiple samples of foraminifera in this study. The Sr isotope dating on benthic foraminiferal species from a single sedimentary unit/single depth allowed the refinement of the existing chronological frameworks. In the present study, foraminifera samples from four shallow borings and one oil well along a transect in the northern North Sea (Fig. 1b) have been investigated to construct a stratigraphical and chronological framework for the Quaternary sediment package. This study builds on work by Sejrup et al. (1987, 1995), here we applied the RP-HPLC method, enabling a more direct comparison with the results of Reinardy et al. (2017, 2018). In addition, this study includes a relatively large number of new Sr ages

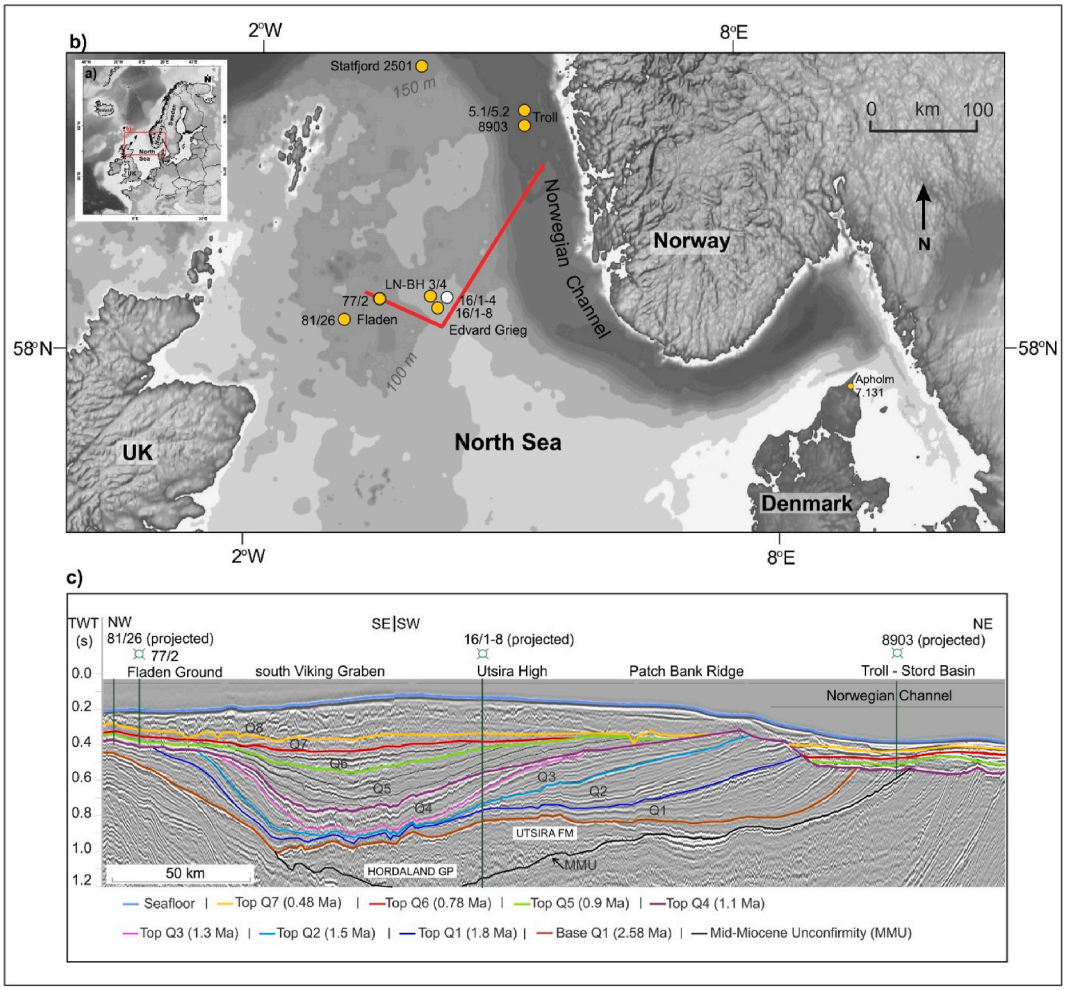

Fig. 1. a) Inset map showing the location of North Sea and surrounding European countries, and the red square indicates the map shown in Fig. 1b. **b)** Map showing the location of a well 16/1–8 and seven shallow borings (yellow circles) studied in the northern North Sea, with the white circle representing location of well 16/1–4 (Eidvin et al., 2020), whose Sr ages from side-wall core samples are discussed in section 5. The red line indicates the location of the seismic profile shown in Fig. 1c. **c)** Seismic profile showing eight Quaternary seismic units (Q1–Q8), Utsira Fm = Utsira Formation and Hordaland Gp = Hordaland Group, where boundaries are marked based on the correlation of regionally continuous reflectors with the well 16/1–8 onto the seismic profile for reference (Baig, 2018) and ages are assigned based on the age-depth model (equation (1)) and D/L Asp calibrated age equation (2), developed in this study. TWT is two-way travel time in second (s).

together with existing data to evaluate the chronology. An attempt has been made to develop an age model based on published Sr ages of the Early Pleistocene sediment package. Using this age model, a tentative age range is assigned to previously marked seismic boundaries in the central North Sea. We developed a regional calibration curve for the extent of racemization of aspartic acid (D/L Asp) in the benthic foraminiferal species, *Elphidium excavatum,* for future use. Based on all the available chronological information, marine oxygen isotope stage (MIS) ages are tentatively assigned to previously identified glacial and interglacial events of the Early and Mid-Pleistocene in the investigated shallow borings. Moreover, a new estimate on the timing of first grounded ice in the central North Sea is proposed. By expanding the geographic extent and integrating the new and existing data, this study aims at improving the existing chronological framework of the Quaternary sediment package in the northern North Sea.

2. Studied material

Benthic foraminiferal species from four shallow borings (81/26, 77/2, LN-BH3/4, 8903) and one well (16/1–8) in a transect from the Fladen Ground to the Troll field in the Norwegian Channel have been investigated (Fig. 1b). In addition, some foraminiferal samples of last interglacial age from borings 5.1/5.2, 7.131, and post-Last Glacial Maximum samples from 2501 and 7.131 have been analyzed by the AAR method for calibration purposes (Table 1; Fig. 1b). By integrating results from AAR analyses and Sr dating with other geochronological evidence, we aim to refine the chronology. It should be emphasized that shallow boring represents sediment units with structures and physical properties intact, and the oil-well samples are from ditch cuttings. The shallow borings and well data have been correlated with high-resolution seismic data, which has allowed for a subdivision of the Quaternary package into eight seismic units (Q1 to Q8; Fig. 1c) (Baig, 2018). The seismic data suggest that the south Viking Graben and Utsira High in Edvard Grieg field represent a part of the basin with a relatively complete Early Pleistocene record preserved (Q1 to Q6). In contrast, the areas to the west and east are identified as the basin margins where Quaternary seismic unconformities are more frequent (Fig. 1c).

Foraminiferal samples for new Sr and AAR analyses from 8903 and 5.1/5.2 (Troll), 2501 (Statfjord), 81/26 (Fladen), and 7.131 (near Apholm, Denmark, presently 3.5 m above sea level) were available at the University of Bergen. New cutting samples from well 16/1–8 were collected from the Norwegian Petroleum Directorate, Stavanger. From shallow boring 5.1/5.2 in the Troll field, only one sample, assumed to represent the Eemian interglacial (MIS 5), based on A/I values and correlation with Eemian sites in western Norway (Sejrup and Knudsen, 1993), was analyzed. For calibration purposes, eight samples representing MIS 2, based on radiocarbon ages, were also analyzed for AAR from the Troll field (8903), Statfjord field (2501) in the northern North Sea, and Apholm (7.131) (Table 1; Fig. 1b). All the depths are presented in meters (m) and denote meters below the seafloor.

2.1. Fladen Ground

The 200.6-m-long shallow boring 81/26 was retrieved from 122 m water depth in the Fladen Ground area (Table 1; Fig. 1b). Sejrup et al. (1987) divided the boring into seven lithological units: three lower marine/glaciomarine units (unit L7 to L5), a till unit (L4), and an upper sequence of three marine/glaciomarine units (L3–L1) (Fig. 2a). Based on foraminiferal stratigraphy and sediment characteristics, the depositional environments were discussed and put into a geochronological framework using radiometric dating and amino acid geochronology based on A/I values of foraminifera, and paleomagnetic investigations. The present study focuses on the units L7 to L5, below the relatively thick till unit, L4, where Stoker et al. (1983) and Sejrup et al. (1987) identified magnetic reversals which they suggested represent the Bruhnes/Matuyama (B/M) with 781 kiloannum (ka) age for the paleomagnetic boundary and the Jaramillo event with 1.07–0.99 million years (Ma) age (Fig. 2a).

The 217.75-m-long shallow boring 77/2 was also retrieved from the Fladen Ground at the water depth of 147 m (Table 1; Fig. 1b). The boring has been divided into seven lithological units, L7 to L1 (Fig. 2b) (King, 1991; Sejrup et al., 1994, 2015; Reinardy et al., 2018) and Stoker et al. (1983) identified the Jaramillo and B/M paleomagnetic boundary. Unit L6 was interpreted as a shallow marine with intervals of glaciogenic material influx; unit L4 and L3 were deposited in marine environments (King, 1991; Reinardy et al., 2018) (Fig. 2b). Two till units L5 and L2 probably represent Mid-Pleistocene and Late Pleistocene glaciations, respectively (King, 1991). The present study presents new (81/26-this study) and unpublished amino acid data (77/2-Reinardy et al., 2017). Likewise, new Sr dates (81/26-this study) and published Sr dates (77/2-Reinardy et al., 2017) from the Fladen cores will focus on the stratigraphy below the two thick till units.

2.2. Edvard Grieg

Oil well 16/1–8 (2067 m deep) was drilled in the Edvard Grieg field at a water depth of 108 m. The stratigraphy of 16/1–8 has been merged with 97 m long shallow boring LN-BH3/4, 10 km to NE from a similar water depth (Reinardy et al., 2017) (Table 1; Figs. 1b and 2c). Note that the 16/1–8 sampling depths reported in Reinardy et al. (2017) are corrected in this study. Samples from 16/1–8 cover the seismic units Q1 to Q4 (Baig, 2018). Based on our new age model, the ages are estimated

Table 1
Details of the shallow borings and a well* discussed in the main text. a.s.l = above sea level and m = meters below seafloor.

Location	Shallow boring/ Well no.	Latitude	Longitude	Water depth (m)	Penetration length (m)	Section/samples analyzed	D/L value	Sr ages	Radiocarbon ages
Apholm	7.131	57°27.80′N	10°31.50′E	3.5 a.s.l	202.6	165 m & 185 m	This study	–	–
Fladen	81/26	58°08.40′N	0°10.63′W	122	200.6	31 m; 100–200 m	This study	This study	–
Fladen	77/2	58°29.5′N	0°30.3′E	147	217.75	10 m; 80–170 m	This study	Reinardy et al. (2018)	–
Edward Grieg	LN-BH3/4	58°50.00′N	2°14.00′E	109	97	0–97 m	This study	Reinardy et al. (2017)	–
Edward Grieg	16/1–8*	58°50.00′N	2°14.00′E	108	2067	277–767 m	This study	This study; Reinardy et al. (2017)	–
Troll	5.1/5.2	60°46.00′N	3°51.00′E	310	150	65 m	This study	This study; Sejrup et al. (1995)	–
Troll	8903	60°38.4′N	3°51.00′E	310	219	15 m; 70–219 m	This study	This study; Sejrup et al. (1995)	Sejrup et al. (1994)
Statfjord	2501	61°17.80′N	1°54.10′E	145.5	120.2	23 m & 53 m	This study	–	–

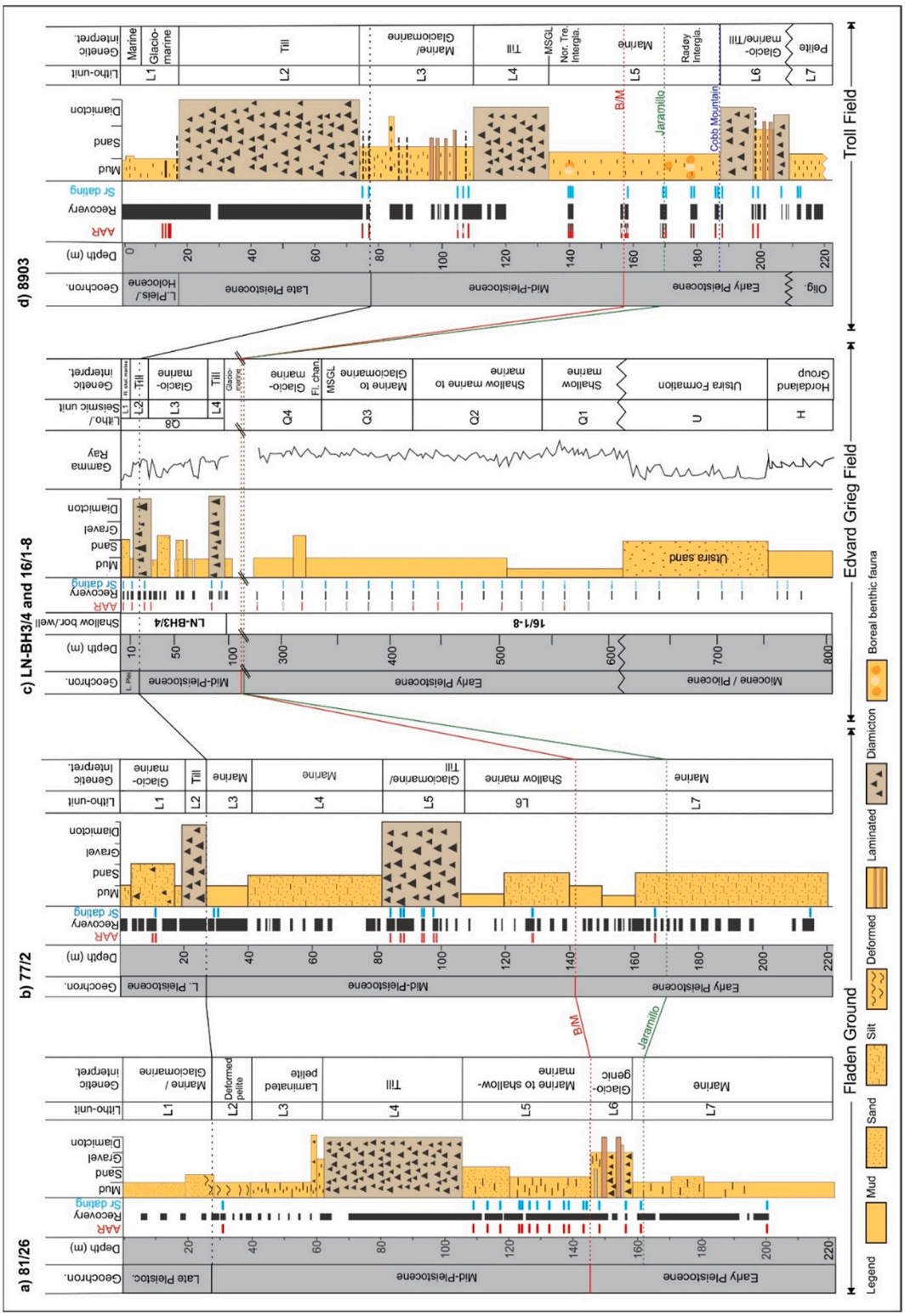

Fig. 2. Lithology logs of four shallow borings and one well investigated along a transect (Fig. 1b) in the northern North Sea from Fladen Ground in the west, the Edvard Grieg field in the middle, and Troll field in the east. Logs modified after **a)** Sejrup et al. (1987) – 81/26; **b)** Reinardy et al. (2017) – 77/2; **c)** Reinardy et al. (2018) – LN-BH3/4 and 16/1–8 and **d)** Sejrup et al. (1995) – 8903. In all the recovery log panel, red bars indicate levels where amino acid analyses were done and blue bars indicate the levels where Sr isotope analyses were done. Depths where multiple foraminifera taxa used for amino acid analysis are marked with a grey bar in 16/1–8 and 8903. Black lines connect the previously published Late Pleistocene boundary and the red dotted line connects the originally marked Mid-Pleistocene boundary in respective shallow borings/well. The Early to Mid-Pleistocene boundary coincides with the B/M paleomagnetic boundary (c. 781 ka) except for LN-BH3/4 where the Mid-Pleistocene boundary is tentative. Green dotted line marks the Jaramillo paleomagnetic boundary (1.07 Ma to 990 ka). In panel **c)** Q1 to Q8 are Quaternary seismic units; U = Utsira Formation; H = Hordaland Group; MSGL = mega scale glacial lineation; Fl. chan. = fluival Channel and Fl. shal. marine = fluvial shallow marine. Notice the change in depth scale and integration of two logs. In panel **d)** Radøy Intergla. = Radøy Interglacial; Nor. Tre. Intergla. = Norwegian Trench Interglacial; MSGL is marked after Rise et al. (2004) and Olig. = Oligocene. Blue dotted line marks the Cobb Mountain event (1.24–1.22 Ma).

for Q1 to Q3 boundaries. Nevertheless, the possibility of an error of ±20 m while picking the seismic reflector for converting the TWT (Two Way Travel-time) to depth should be emphasized. Shallow boring LN-BH3/4 penetrating seismic unit Q8 has been subdivided into four main lithological units (L4–L1), where L4 and L2 are till units and, L3 and L1 represent glaciomarine to marine environments (Reinardy et al., 2017) (Fig. 2c). In this study, unpublished AAR data from 16/1–8 and LN-BH3/4 and published Sr ages of foraminifer were used to refine the chronology of the Early and Mid-Pleistocene. Additionally, shell fragment samples between 767 m and 567 m have been analyzed for Sr isotopes to extend the chronological control deeper from the assumed base of the Quaternary (612 m) to the Utsira Formation (747–612 m) in the Nordland Group and the boundary of Hordaland Group (Figs. 1b and 2c).

2.3. Troll

The 219-m-long shallow boring 8903 was retrieved at the water depth of 320 m from the Troll field in the Norwegian Channel (Table 1; Fig. 1b). Recovery of the top 70 m section was continuous, and below that, it was *c.* 25% (Fig. 2d). The shallow boring was subdivided into seven lithological units (L7–L1) and was dated by radiocarbon and amino acid geochronology (A/I values) in foraminifera, Sr dates (foraminifera and mollusc), paleomagnetism, and biostratigraphy (Sejrup et al., 1994, 1995) (Fig. 2d). Unit L7 represents an inner shelf – lagoonal environment of Oligocene age. The diamicton (L6) above the Oligocene sediments is named the Fedje Till and is considered as the earliest sedimentological evidence of grounded ice in the North Sea, dated to around 1.1 Ma (Sejrup et al., 1995). Unit L5 represents marine conditions, where, based on foraminiferal biostratigraphy, two interglacial events were identified: the Radøy Interglacial and Norwegian Trench Interglacial (Sejrup et al., 1989; Sejrup and Knudsen, 1993). Till unit L4 was deposited during one or more of the Mid-Pleistocene glaciations, whereas till unit L2 possibly represent multiple advances of the Fennoscandian ice sheet during MIS 4-2 (Sejrup et al., 1995). Unit L3 and L1 indicate marine to glaciomarine conditions. In this study, new AAR and Sr analyses are performed on foraminifera samples from 8903 to refine the chronology of unit L6 to L4 (Fig. 2d). From the shallow boring 5.1/5.2, west of 8903, amino acid analyses of foraminifera sampled from the sediments of possible Eemian age, partly corresponding to L3 in 8903 (Sejrup et al., 1989), have been performed.

3. Methods

3.1. Strontium isotope dating

Strontium isotope dating is based on the assumption that $^{87}Sr/^{86}Sr$ values measured in carbonate marine fossils reflect the seawater composition at the time of their test formation (Kuznetsov et al., 2012). Changing Sr ratios of seawater with time makes it possible to derive the ages of marine carbonate fossils from a global calibration curve (Howarth and McArthur, 1997; McArthur et al., 2001). In this study, 88 mono-specific and three mixed foraminiferal samples were selected from 81/26, 8903, and 5.1/5.2, and nine shell fragment samples from 16/1–8 were analyzed for Sr isotope dating (Table 2 and Appendix A). When possible, foraminifera samples for Sr dating were picked from the same depth as AAR samples.

Samples containing 20–60 foraminifera were placed in pre-cleaned 2 ml polypropylene centrifuge tubes and 1 ml of a 0.1 M HCl was added. The samples were then left to dissolve in the acid for 12 h. Subsequently, the samples were centrifuged at 10000 rpm for 5 min; the HCl supernatant was transferred to small PFA beakers and evaporated to dryness on a heating plate at 60 °C. The residue was dissolved in small amounts of 3 N HNO_3, typically 0.5–1 ml, and Sr was separated by specific extraction chromatography on Sr-spec resin using a modified version of the method described by Deniel and Pin (2001). The Sr eluates were collected in 2 ml micro-centrifuge tubes and evaporated until dry. We measured Sr isotopes on a Finnigan 262 mass-spectrometer at the Department of Earth Science, University of Bergen, and corrected Sr isotopic ratios for mass fractionation using an $^{87}Sr/^{86}Sr$ value of 8.375209. Repeated measurements SRM 987 Strontium Carbonate standard at the time of analyses yielded an average $^{87}Sr/^{86}Sr$ value of 0.710235 ± 0.000009 (2σ) ($n = 10$) and the measured $^{87}Sr/^{86}Sr$ values are corrected to 0.710240.

Based on the availability of benthic foraminifera, multiple species were analyzed from a single depth, and $^{87}Sr/^{86}Sr$ values were converted to numerical ages using the calibration curve V3:10/99 by McArthur et al. (2001). Earlier published Sr ages for 8903 (Sejrup et al., 1995) were calibrated using curves by DePaolo (1986), Hess et al. (1986), and DePaolo and Ingram (1985) with $2\sigma = 0.000031$. Reinardy et al. (2018) presented re-calibrated Sr ages for the shallow boring 8903 using McArthur et al. (2001). One Sr age at 219 m (30.87 Ma) is concordant with new Sr dates, whereas the other re-calibrated dates are distinctly older (published ages by Sejrup et al., 1995 are marked with asterisk* in Table 2 and Appendix A).

A two-step processing, i.e., screening, and averaging have been applied on Sr data. In the first screening step, 12 $^{87}Sr/^{86}Sr$ values which were higher than the upper limit of the Sr calibration curve (*i.e.,* > 0.709175 = zero, denoting modern sample) were excluded. On converting the remaining $^{87}Sr/^{86}Sr$ values to numerical ages, an additional 17 Sr ages were excluded, which were distinctly too old or young either in a set of ages from the same depth level or the same lithological unit (indicated with bold in Appendix A). In the second step, to get clarity in the trend of downcore Sr ages, multiple Sr ages which are (i) from the same depth but measured on different foraminifera species and (ii) from a similar depth (within 0.1–2.0 m sampling interval), and the same lithological unit and have a similar Sr age (±0.2 Ma) have been combined and averaged. Both steps are also applied to previously published Sr ages from shallow boring 77/2. In 16/1–8, a single analysis was done for each depth level at intervals of 20 m, hence screening and averaging were not applied. All the published Sr ages are included in Table 2, together with processed Sr ages of remaining shallow borings. The complete list of unprocessed Sr ages is given in Appendix A.

An age model is prepared using previously published Early Pleistocene Sr ages of the Quaternary sediment package in well 16/1–8 (Reinardy et al., 2018) (Fig. 3). It was challenging to include all Sr ages around the onset of the Quaternary in one regression curve. Hence, new Sr ages below the Quaternary, from the Utsira Formation and the Hordaland Group, are not included in the preparation of the age-depth model. Using the LINEST function (Morrison, 2015), the coefficients of 4th order polynomial equation ($y = a4x^4 + a3x^3 + a2x^2 + a1x + a0$) are calculated, from measured Sr ages (y) and corresponding depths (x) -

$$A = (0.000000001168 * d^4) + (-000002015601 * d^3) + (0.001285436544 * d^2) + (-0.356465307704 * d) + (37.522222589829) \quad (1)$$

where, A = age in Ma and d = depth in meters below the seafloor.

To calculate the uncertainty range of the polynomial equation (1), the LINEST function by Morrison (2015) is used on the uncertainty range of Sr age. The two equations defining the maximum and minimum range of the polynomial regression curve are given in Appendix B.

3.2. Amino acid racemization

Amino acids, the building blocks of protein, are present in the L– form ('levo' or left-handed isomer) in living organisms. Upon the death of an organism, the L– form starts converting to D– form (dextro or right-handed isomer). This phenomenon of conversion is termed racemization (epimerization for isoleucine), and the extent of racemization is given as the ratio between the D and L form (D/L). The D/L value is influenced by temperature history, taxonomy, age of the fossil, and environmental factors (Miller and Brigham-Grette, 1989; Kaufman et al., 2013;

Table 2
D/L Asp (aspartic acid), D/L Glu (glutamic acid) and strontium (Sr) ages for all the shallow borings and well. The D/L values with ±1 sigma (±1σ) and Sr ages (in Ma) with minimum (Min) and maximum (Max) ages presented. Corrected $^{87}Sr/^{86}Sr$ values are converted to Sr ages using the calibration curve by McArthur et al. (2001). D/L values and Sr ages in this table are averaged values and are used in Fig. 6. For details on averaging refer to the Methods section in the main text. All ages marked with an (*) asterisk in 8903 are from Sejrup et al. (1995) and those written in bold are older ages/reworked ages. Refer Appendix A for complete dataset of $^{87}Sr/^{86}Sr$ values and Sr ages before averaging and 2S error in Sr isotope analysis. Refer Appendix C for a complete dataset of amino acid ratios including D/L values of all eight amino acids, CV (coefficient of variance) and standard deviation. Litho/seismic units are based on Fig. 2.

Mean Depth (m)	Unit	Benthic foraminifera species	Sample ID avgd.	No. of samples avgd.	Total sub-samples | Sub-sample rejected	Mean D/L Asp	Mean D/L Asp ± 1σ	Mean D/L Glu	Mean D/L Glu ± 1σ	Sample ID avgd.	No. of samples avgd.	Min.	Mean Sr age (Ma)	Max.
Apholm - 7.131 *(D/L values - This study)*														
165.7		*Bulimina marginata*	19208	1	8 | 1	0.396	0.023	0.179	0.019					
185.0		*Bulimina marginata*	19209	1	6 | 0	0.379	0.025	0.169	0.019					
Fladen Ground - 81/26 *(D/L values; Sr age - This study)*														
31.6	L2	*Elphidium excavatum*	16938	1	7 | 0	0.450	0.032	0.210	0.037	8923, 8924	2	0.33	0.39	0.47
109.7	L5	*Elphidium* spp.	16939	1	3 | 0	0.590	0.044	0.354	0.060	8925	1	1.14	1.18	1.23
114.5	L5	*Elphidium* spp.	16940	1	2 | 0	0.619		0.407		8926	1	0.95	1.04	1.09
118.7	L5	*Elphidium excavatum*	16941	1	6 | 3	0.520	0.041	0.229	0.025	8927, 8928	2	1.09	1.14	1.19
124.0	L5	*Elphidium excavatum*								8929, 8930, 8951, 8952, 8953, 8954	6	1.12	1.18	1.23
122.5	L5	*Elphidium excavatum*	16942, 16943, 16944, 16945	4	25| 5	0.574	0.036	0.290	0.057					
129.1	L5	*Elphidium excavatum*								8955, 8956, 8957	3	1.06	1.13	1.19
133.1	L5	*Elphidium excavatum*	16946	1	6 | 1	0.540	0.017	0.203	0.006	8958, 8959, 8960	3	1.18	1.23	1.27
138.8	L5	*Elphidium excavatum*	16947, 16948	2	7 | 1	0.573	0.051	0.297	0.068					
138.8	L5	Mixed benthic								8931, 8932, 8933	3	1.17	1.22	1.26
143.5	L5	*Elphidium excavatum*	16949	1	3 | 0	0.597	0.043	0.321	0.071	8934	1	0.98	1.05	1.10
144.5	L5	*Uvigerina peregrina*								8935, 8936	2	0.79	0.88	0.95
147.7	L6	Mixed benthic								8937, 8938, 8939, 8940, 8941	5	1.05	1.10	1.15
148.0	L6	*Elphidium excavatum*	16952	1	6 | 1	0.653	0.052	0.442	0.093					
156.6	L6	*Elphidium excavatum*	16953	1	6 | 0	0.619	0.022	0.328	0.036	8942, 8943	2	1.25	1.30	1.35
161.3	L7	*Elphidium excavatum*	16954	1	6 | 2	0.640	0.022	0.383	0.042	8945, 8946	2	1.22	1.27	1.31
200.3	L7	*Elphidium excavatum*	16955	1	4 | 1	0.633	0.014	0.386	0.039					
200.3	L7	Mixed benthic								8947, 8949, 8950	3	1.18	1.23	1.27
10.5	L1	*Elphidium excavatum*	10939, 10940	2	16 | 1	0.377	0.022	0.125	0.017					
33.2	L3	*Elphidium excavatum*								7577	1	0.30	0.35	0.42
87.4	L5	*Elphidium excavatum*	10941, 10942, 10943	3	25 | 2	0.588	0.038	0.290	0.053	7579, 7580, 7581	3	0.46	0.53	0.60
95.8	L5	*Elphidium excavatum*	10944, 10945	2	16 | 4	0.570	0.040	0.290	0.047					
97.2	L5	*Elphidium excavatum*								7583, 7584, 7585	3	0.49	0.55	0.62
99.5	L5	*Elphidium excavatum*	10946, 10947	2	18 | 3	0.599	0.041	0.305	0.051					
130.5	L6	*Elphidium excavatum*	10948, 10949	2	18 | 3	0.653	0.024	0.374	0.037	7586, 7587	2	0.92	1.01	1.08
157.1	L7	*Elphidium excavatum*								7588	1	0.66	0.74	0.82

(*continued on next page*)

Table 2 (*continued*)

Mean Depth (m)	Unit	Benthic foraminifera species	Sample ID avgd.	No. of samples avgd.	Total sub-samples | Sub-sample rejected	Mean D/L Asp	Mean D/L Asp ± 1σ	Mean D/L Glu	Mean D/L Glu ± 1σ	Sample ID avgd.	No. of samples avgd.	Min.	Mean Sr age (Ma)	Max.
166.4	L7	*Elphidium excavatum*	10950	1	8 | 0	0.688	0.012	0.458	0.036	7589	1	0.98	1.05	1.10
215.0	L7	*Elphidium excavatum*								7590	1	1.38	1.42	1.48
5.4	L1	*Elphidium excavatum*	10951	1	10 | 1	0.369	0.010	0.092	0.012					
14.5	L2	*Elphidium excavatum*	10952	1	7 | 1	0.407	0.021	0.149	0.014	7591	1	0.11	0.15	0.20
25.0	L2	*Elphidium excavatum*	10953	1	9 | 1	0.460	0.030	0.196	0.027					
38.8	L3	*Elphidium excavatum*	10954	1	9 | 0	0.477	0.027	0.209	0.027					
51.4	L3	*Elphidium excavatum*								7593	1	0.03	0.07	0.11
84.0	L4	*Elphidium excavatum*	10955	1	10 | 0	0.538	0.056	0.246	0.069	7594	1	1.05	**1.10**	1.14
97.0	L4	*Elphidium excavatum*								7595	1	0.09	**0.12**	0.17
277	Q4	*Elphidium excavatum*	12384	1	9 | 0	0.727	0.037	0.526	0.079					
307	Q4	*Cassidulina laevigata*								7755	1	1.26	1.31	1.36
327	Q4	*Elphidium excavatum*	12387	1	8 | 0	0.777	0.030	0.611	0.050					
327	Q4	*Cassidulina laevigata*								7756	1	1.28	1.32	1.37
347	Q3	*Elphidium excavatum*								7757	1	1.22	1.27	1.31
367	Q3	*Elphidium excavatum*								7758	1	1.18	1.23	1.28
387	Q3	*Elphidium excavatum*								7759	1	1.38	1.42	1.48
407	Q3	*Cassidulina laevigata*								7760	1	1.55	1.66	1.77
427	Q2	*Elphidium excavatum*	12518	1	6 | 1	0.729	0.049	0.587	0.096	7761	1	1.76	1.87	2.01
447	Q2	*Elphidium excavatum*	12519	1	5 | 0	0.845	0.030	0.756	0.070					
447	Q2	*Cassidulina laevigata*								7762	1	1.43	1.49	1.57
467	Q2	*Elphidium excavatum*	12521	1	9 | 2	0.826	0.022	0.740	0.065					
467	Q2	*Cassidulina laevigata*								7763	1	1.38	1.42	1.48
487	Q2	*Cassidulina laevigata*								7764	1	1.70	1.81	1.92
507	Q2	*Elphidium excavatum*	12527	1	4 | 0	0.801	0.012	0.702	0.059					
507	Q2	*Cassidulina laevigata*								7765	1	1.41	1.47	1.54
527	Q2	*Cassidulina laevigata*								7766	1	1.89	2.02	2.14
547	Q1	*Cassidulina laevigata*								7767	1	1.49	1.57	1.68
567	Q1	*Elphidium excavatum*	12527	1	7 | 1	0.820	0.037	0.740	0.078					
567	Q1	Shell fragments								9121	1	1.35	1.40	1.45
567	Q1	*Melonis barleeanus*								7768	1	2.17	2.27	2.40
587	Q1	*Melonis barleeanus*								7769	1	2.43	2.57	3.22
607	Q1	*Melonis barleeanus*								7770	1	2.23	2.34	2.47
607	Q1	Shell fragments								9122	1	2.32	2.44	2.61
627	U	Shell fragments								9123	1	4.04	4.30	4.56
657	U	Shell fragments								9124	1	6.09	6.14	6.22
687	U	Shell fragments								9125	1	15.26	15.48	15.67

(*continued on next page*)

Table 2 (*continued*)

Mean Depth (m)	Unit	Benthic foraminifera species	Sample ID avgd.	No. of samples avgd.	Total sub-samples | Sub-sample rejected	Mean D/L Asp	Mean D/L Asp ± 1σ	Mean D/L Glu	Mean D/L Glu ± 1σ	Sample ID avgd.	No. of samples avgd.	Min.	Mean Sr age (Ma)	Max.
707	U	Shell fragments								9126	1	16.09	16.25	16.39
727	U	Shell fragments								9127	1	12.35	12.76	13.09
757	H	Shell fragments								9128	1	16.31	16.44	16.56
767	H	Shell fragments								9129	1	16.27	16.41	16.53
65.5		*Cassidulina laevigata*								8879	1	0.11	0.15	0.20
65.5		*Uvigerina pregrina*	16936	1	7 | 4	0.220	0.010	0.171	0.014					
65.5		*Bulimina marginata*	16937	1	9 | 7	0.248	0.024	0.220	0.019				**0.00***	
65.5		*Elphidium excavatum*											**0.00***	
14.6	L2	*Elphidium excavatum*	19202, 19203, 19204, 19205	4	34 | 2	0.297	0.010	0.078	0.006					
73.7	L2	*Elphidium excavatum*	16891, 16892	2	11 | 0	0.500	0.029	0.192	0.022					
77.5	L3	*Elphidium excavatum*	16894	1	5 | 0	0.580	0.012	0.287	0.019					
77.5	L3	Mixed benthic								8881, 8882	2	0.31	0.37	0.45
107.8	L3	*Elphidium excavatum*	16896, 16900, 16901	3	15 | 2	0.590	0.024	0.290	0.030					
138.4	L5	*Bulimina marginata*									1	2.23	**2.34***	2.47
138.4	L5	*Elphidium excavatum*									1	1.52	**1.62***	1.73
140.2	L5	*Elphidium excavatum*	16902, 16905, 16907	3	14 | 4	0.595	0.026	0.288	0.037					
140.4	L5	Mixed benthic								8892, 8895, 8896, 8898, 8899, 8900, 8902	7	0.45	0.51	0.59
157.6	L5	*Elphidium excavatum*	16911	1	5 | 1	0.629	0.033	0.304	0.054					
158.8	L5	*Elphidium excavatum*	16914, 16917	2	12 | 0	0.565	0.034	0.246	0.042					
158.9	L5	Mixed benthic								8871,8872, 8873,8875	4	0.53	0.60	0.68
169.5	L5	*Bulimina marginata*									1	4.41	**4.64***	4.80
169.5	L5	*Elphidium excavatum*									1	1.21	**1.25***	1.30
169.8	L5	Mixed benthic								8916, 8918, 8919	3	0.58	0.65	0.73
170.6	L5	*Elphidium excavatum*	16923	1	4 | 1	0.620	0.006	0.280	0.011					
179.3	L5	Mixed benthic								8889, 8921, 8922	3	0.67	0.75	0.83
188.3	L6	Mixed benthic	16928, 16930, 16931	3	13 | 5	0.665	0.020	0.376	0.039	8913, 8903, 8904, 8906	4	0.85	0.92	0.99
198.7	L6	*Elphidium* spp.								8908	1	0.85	0.96	1.04
199.0	L6	*Elphidium excavatum*	16934, 16935	2	9 | 0	0.678	0.024	0.371	0.034					
201.0	L6	*Elphidium excavatum*									1	5.90	**5.95***	5.99
207.0	L6	Mixed Benthic								8910	1	23.06	**23.25**	23.42
212.0	L7	Mixed Benthic								8911	1	26.18	26.41	26.65
213.0	L7	Mixed Benthic								8912	1	32.85	33.00	33.18

(*continued on next page*)

Table 2 (*continued*)

Mean Depth (m)	Unit	Benthic foraminifera species	Sample ID avgd.	No. of samples avgd.	Total sub-samples | Sub-sample rejected	Mean D/L Asp	Mean D/L Asp ± 1σ	Mean D/L Glu	Mean D/L Glu ± 1σ	Sample ID avgd.	No. of samples avgd.	Min.	Mean Sr age (Ma)	Max.
219.0	L7	Alabamina sp.									1	30.63	30.87*	31.12
Statfjord - 2501 ***(D/L values - This study)***														
23.0		*Elphidium excavatum*	19206	1	4 | 0	0.306	0.025	0.088	0.008					
53.0		*Bulimina marginata*	19207	1	5 | 1	0.401	0.027	0.160	0.008					

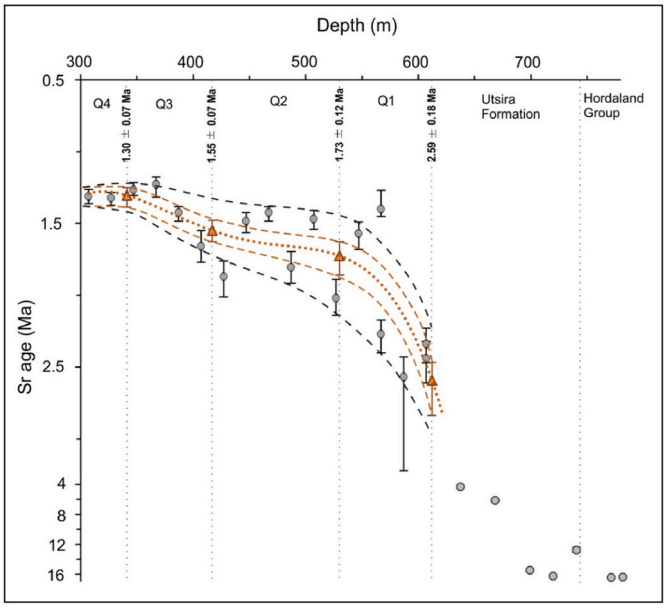

Fig. 3. An age-depth model (dotted orange curve) is constructed based on Sr ages (in Ma) of the Early Pleistocene sediment from well 16/1–8 using a 4th order polynomial regression curve. Sr ages with error bars (grey circle) representing the Early Pleistocene sediment from units Q1 to Q3 and part of Q4 are included in model; Sr ages with error representing Miocene/Pliocene sediment covering the Utsira Formation and the Hordaland Group are not included in model. Note the change in Sr age scale in y-axis. The ages assigned to the Quaternary seismic boundary depths, Q1 to Q3, and the age derived at the boundary between the Utsira Formation and the Early Pleistocene, representing the base-Quaternary at 612 m (~2.59 ± 0.18 Ma) (orange triangle with error bar), are based on the equation of the polynomial curve (*refer* equation (1)) from this study. Inner orange dashed lines envelop the uncertainty range for the age-depth model (coefficients of equations for calculating the ages and their uncertainty are given in Appendix B) and outer grey dashed lines envelop the uncertainty range for Sr ages.

Kaufman, 2014). Within a region or setting with similar temperature history, a calibration curve based on D/L values derived from samples of the same taxon and independent dates may be used to estimate a numerical age or assign a relative age to the sample (Sejrup et al., 1984; Kaufman et al., 2008, 2013). Based on A/I values derived from amino acid analyses of foraminiferal samples from dated levels in different parts of the northern North Sea and downcore temperature measurements, it has been suggested that the investigated sediments sampled in this study have been exposed to similar temperature histories through the Quaternary (Harper, 1971; Evans and Coleman, 1974; Reinardy et al., 2018).

Seventy-four new mono-specific foraminifer samples (*Elphidium excavatum, Elphidium* sp., *Cassidulina laevigata, Bulimina marginata, Melonis barleeanus, Uvigerina peregrina, Islandiella islandica)* were analyzed from shallow borings 81/26 (19 samples), 8903 (49 samples), 5.1/5.2 (2 samples), 2501 (2 samples) and 7.131 (2 samples) constituting a total of 386 subsamples (Appendix C). Here, a 'sample' contains 80 to100 foraminifera picked from one depth interval, and 'subsample' is a split of one sample into 5–10 subsamples, each containing 10–15 foraminifera. Using RP-HPLC, eight D/L values (aspartic acid = Asp; glutamic acid = Glu; serine = Ser; alanine = Ala; valine = Val; phenylalanine = Phe; isoleucine = Ile and leucine = Leu) from amino acid racemization are measured. Previously, Reinardy et al. (2017, 2018) analyzed a total of 37 samples of mono-specific *Elphidium excavatum* and *Cassidulina laevigata* from 77/2 (13 samples), LN-BH3/4 (5 samples), and 16/1–8 (19 samples) using RP-HPLC, as in the present study, but presented only the D/L Ile values. A complete data set of eight amino acids analyzed in multiple foraminifera species is provided in Appendix C and D and D/L Asp and D/L Glu values measured in *Elphidium excavatum* are included in Table 2.

Based on availability, multiple species were analyzed with the RP-HPLC method. Each sample (80–100 foraminifers) was cleaned by immersion in 1 ml of 3% H_2O_2 for 2 h and then rinsed with deionized water three times. Subsequently, the sample was subdivided into 5–10 subsamples, and each subsample containing 10–15 foraminifers of the same species was dissolved in 7 μl of 6M HCl, sealed under N_2 (nitrogen gas), and hydrolyzed at 110 °C for 6 h. After this, the samples were evaporated in a desiccator for 24 h. Before injecting the sample onto the RP-HPLC, it was rehydrated with 4 μl of L-*homo*arginine, which was used as an internal spike to quantify the abundance of amino acids. The instrumentation and procedures are described in Kaufman and Manley (1998) and Kaufman (2000). The samples were analyzed at the Amino Acid Geochronology Laboratory (AAGL), Northern Arizona University, Flagstaff, USA.

To exclude possible contaminated samples, the steps suggested by Sejrup and Haugen (1992), Kosnik and Kaufman (2008), and Kaufman et al. (2013) were applied on 113 samples (671 subsamples). The three steps are followed: a) subsamples with concentration ratios of [L-Ser]/[L-Asp] above 0.8 were rejected; b) subsamples with D/L Asp or Glu values falling outside the range of ± 2σ of other subsamples were rejected; and c) cross-plot between D/L Asp and D/L Glu are evaluated to examine the internal consistency and identify off-trend samples (Fig. 4a). Consequently, 49 subsamples of *Elphidium excavatum* out of 401 subsamples (12%) were rejected, and 126 subsamples of the other species out of 270 subsamples (47%) were rejected. Screening of AAR results shows that the proportion of rejected samples depends on the taxon, where most of the excluded data were of *Cassidulina laevigata (26%), Bulimina marginata (61%), Uvigerina peregrina (74%), Melonis barleeanus (67%),* and *Islandiella islandica (83%)* species, and fewer rejections were made in results from *Elphidium excavatum (12%)* (Appendix D). A cross-plot of D/L Asp and D/L Glu values shows a tighter covariance in *Elphidium excavatum* compared to other species

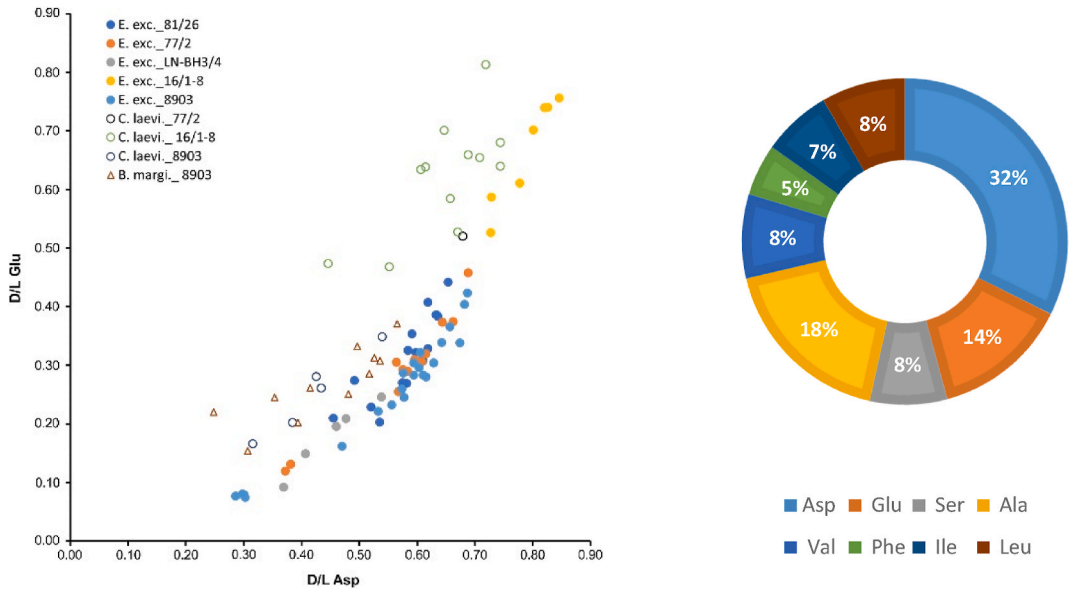

Fig. 4. a) Co-variance between D/L Asp and D/Glu in three species (*E. exc.* = *Elphidium excavatum, C. laevi.* = *Cassidulina laevigata* and *B. margi.* = *Buliminia marginata*) measured in four shallow borings (81/26; 77/2; LN-BH3/4 and 8903) and one well (16/1–8) **b)** Relative concentration of eight amino acids measured in individual subsamples of benthic foraminifera *Elphidium excavatum* before screening.

(Fig. 4a). Hence, we used only results of *Elphidium excavatum* further.

Likewise, the racemization in five amino acids, Asp, Glu, Ala, Val, and Ile in *Elphidium excavatum* showed reasonable results and relative concentration ranging from 32% to 5% (Fig. 4b). Both Asp and Glu are suitable to refine the chronology. In addition, the relatively slow racemizing Glu has potential to resolve age difference in older samples and possibly identify compromised samples. However, in this study, Asp constitutes the highest abundance of *c.* 32% of the total hydrolysable amino acids in the *Elphidium excavatum* before screening (Fig. 4b) and after screening Asp constitutes *c.* 30% where most of the subsamples were rejected because of high Ser concentration indicating modern contamination (Appendix C) (Miller and Brigham-Grette, 1989; Kosnik and Kaufman, 2008). Thus, due to higher abundance of Asp in all *Elphidium excavatum* samples and its lower intra-sample variability, D/L Asp values are more reliable and, we have opted D/L Asp values in *Elphidium excavatum* for calibration.

After excluding the outliers, the samples of *Elphidium excavatum* from the same lithological unit with similar D/L Asp values (≤0.02 difference) and within a 1 m sampling interval have been averaged. These averaged D/L values are used in plotting graphs of respective shallow borings. Reinardy et al. (2017) used D/L Ile values from both *Elphidium excavatum* and *Cassidulina laevigata* for interpretation, whereas, in this paper we have focused on D/L Asp values in *Elphidium excavatum* for interpretation and calibration (Table 2). The complete dataset of all amino acid analyses is provided in Appendix C, which also includes standard deviation (S.D.) and Coefficient of Variation (CV) = (S.D./Mean of D/L values) x 100.

We calibrate the extent of Asp racemization in *Elphidium excavatum* using three tie points with well-constrained independent ages (Table 3; Fig. 5). The top of Utsira Formation, assumed to represent the base-Quaternary (2.58 Ma), is marked at 612 m in 16/1–8. The first available D/L Asp value above this boundary, from 567 m (0.82 ± 0.037) and Sr age of 2.28 ± 0.1 Ma, is used as the oldest calibration point (Fig. 5a and b). Previous workers identified the B/M paleomagnetic reversal (Early to Middle Pleistocene boundary) in three shallow borings (81/26, 77/2 and 8903 - Stoker et al., 1983; Sejrup et al., 1987, 1995). The D/L Asp values at/close to the B/M boundary are similar (0.65 ± 0.052) in all the three shallow borings; therefore, an age of 781 ka is assigned to this D/L value. The mean D/L Asp value (0.30 ± 0.01) in four samples from 8903 and one sample from 2501 corresponds to a radiocarbon age of ~15 ka (Sejrup et al., 1994) and is used as the youngest calibration point (Fig. 5b). Using the power regression equation of tie-points, ($y = 0.6900x^{0.2033}$; Fig. 5b), the age equation for D/L Asp value is -

$$A = 6.2{*}D/L^{4.92} \quad (2)$$

where, A = age in Ma and D/L = D/L Asp value.

The ages are obtained for all D/L Asp values using equation (2) and correlated with Sr ages at the same depth (Fig. 5c). This generalized calibrated age equation (2) can be applied elsewhere in the North Sea, where similar temperature history can be assumed.

Table 3
Details of the amino acid ratio and age tie-points used for calibration of D/L Asp (aspartic acid) in *Elphidium excavatum*.

D/L Asp	Age (Ma)	Age tie-points	Age tie-point reference
0.30 ± 0.023	0.015 ± 0.002	^{14}C age	Sejrup et al. (1994)
0.65 ± 0.025	0.781	Brunhes/Matuyama paleomagnetic boundary	Sejrup et al. (1987,1995), Stoker et al. (1983)
0.82 ± 0.037	2.2 ± 0.1	Strontium (Sr) age	This study

4. Results and interpretations

4.1. Sr isotope dating

In 81/26 from the Fladen Ground, Sr ages cover the period from 1.3 Ma to 380 ka, indicating an Early to Mid-Pleistocene age (Table 2; Fig. 6a). Unit-L6 falls between the Jaramillo and the B/M paleomagnetic boundary suggesting an age range from 990 ka to 781 ka; however, the Sr ages from L5 show relatively older ages (1.3–1.1 Ma). A Sr age of 880 ± 100 ka close to the B/M boundary at unit L6/L5 transition supports the chronological framework suggested by Sejrup et al. (1987). The somewhat older ages obtained in unit-L5 may result from stronger river influence in a shallow-water depositional environment (*e.g.,* Kaufman et al., 1993) or windblown dust or coastal groundwater (Evans et al., 2010; El Meknassi et al., 2018). Micropaleontological and the lithological evidence from unit-L5 in 81/26 suggests that these sediments were deposited from 10 to 0 m water depth in a shallow fluvial environment

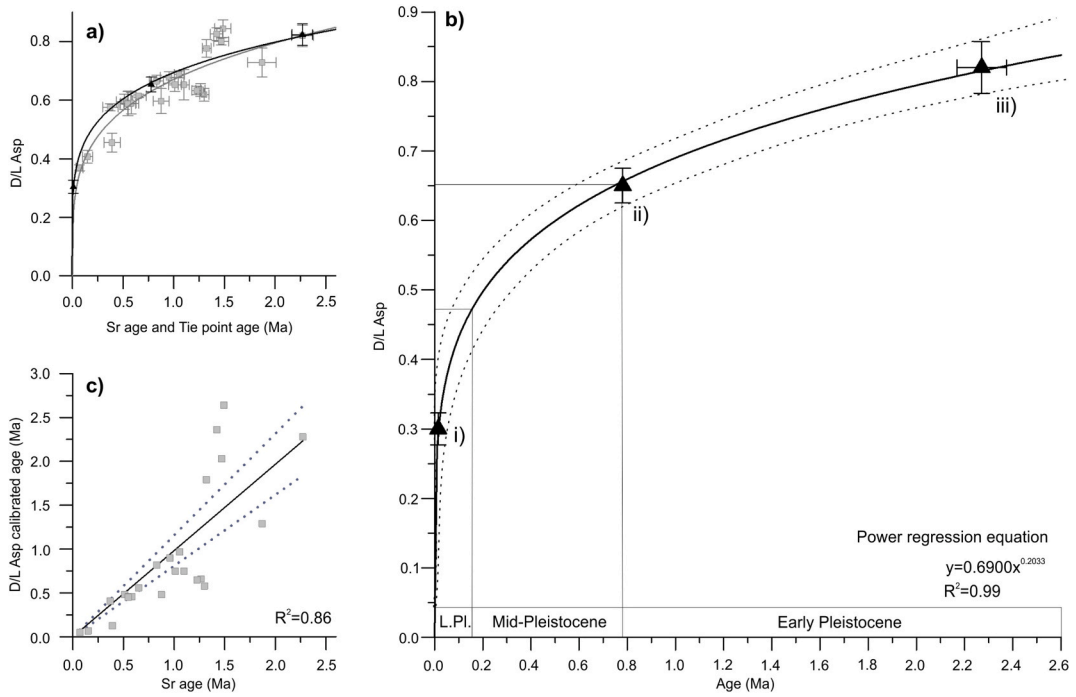

Fig. 5. a) D/L Asp *vs* Sr age with power regression curve (in grey) and the calibration curve (in black) superimposed **b)** Calibration curve of D/L Asp values (black curve) based on three age tie points (triangle with error bar): (i) calibrated radiocarbon age, (ii) Bruhnes/Matuyama (B/M) paleomagnetic boundary and (iii) Sr age (*refer* Table 3 for details); grey dotted curve envelops the standard deviation of D/L Asp values; grey line shows the boundary of the Late and Mid-Pleistocene **c)** Correlation of Sr age and D/L Asp calibrated ages at the same depth. The ages are estimated for the same D/L Asp values which are used in the first panel.

(Sejrup et al., 1987). The source of freshwater was most likely from the eastern part of Britain, which comprises Carboniferous Limestone with a low Sr isotope ratio of 0.709 (Evans et al., 2010); weathering of these underlying rocks probably influences the isotopic composition of the rivers. Previously published Sr ages (Reinardy et al., 2018) from the other Fladen core (77/2) range from 1.42 Ma to 800 ka (Table 2; Fig. 6b) and generally support the dates from the same seismic units in shallow boring 81/26.

In 16/1–8 from the central basin, the top of the Hordaland Group is located at 747 m below the seafloor, and the two similar Sr ages from this unit, 16.4 ± 0.1 Ma, suggest a Miocene age (Table 2; Fig. 6c). Five Sr ages within the Utsira Formation (747–612 m) range from 16.2 ± 0.4 Ma to 4.3 ± 0.3 Ma (Fig. 6c). The assumed base of the Quaternary boundary between U and seismic unit Q1 is marked at 612 m. At 607 m, a Sr age from shell fragment equals 2.4 ± 0.2 Ma (Fig. 6c). This age is in-line with previously published Sr age from foraminifera at 607 m, 2.3 ± 0.1 Ma (Reinardy et al., 2017). The other published Sr ages between 607 m and 307 m range from 2.3 to 1.2 Ma, and four published Sr ages in LN-BH3/4 (97–0) range between 1.1 Ma and 120 ka (Table 2; Fig. 6c).

In 8903 from the Norwegian Channel, the bottom two new Sr ages, 33 ± 0.2 Ma, and 26.41 ± 0.2 Ma, from unit-L7 agrees with biostratigraphic evidence and one earlier Sr date (30.87 ± 0.2 Ma) suggesting an Oligocene age (Sejrup et al., 1995) (Table 2; Fig. 6d). In unit-L6, a published Sr age, 5.95 ± 0.05 Ma and new Sr age 23.25 ± 0.2 Ma could represent reworking by glacial processes from sediments below the angular unconformity (Sejrup et al., 1995). The remaining Sr ages between 199 and 77 m range from ~1 Ma to 300 ka, representing the Early to Mid-Pleistocene sediments deposited above the unconformity (Table 2; Fig. 6d). The new Sr ages of unit-L5 generally support the interpretation of the paleomagnetic data presented by Sejrup et al. (1995), where the B/M boundary was marked at *c.* 157 m and two events in the Matuyama Chron – Jaramillo (0.99 Ma) and Cobb Mountain (1.2 Ma), were marked at *c.* 169 m and *c.* 188 m, respectively (Fig. 2d). However, an offset of the Sr ages relative to the paleomagnetic datum levels may be attributed to the low core recovery. Moreover, an approximated similar D/L Asp value of 0.65 ± 0.03 is documented in all three shallow borings around the B/M boundary (Fig. 6a, b and 6d).

Previously, two samples assumed to represent the last interglacial period were analyzed from the neighbouring shallow boring 5.1/5.2 (Fig. 1a) (Sejrup et al., 1989, 1995), where $^{87}Sr/^{86}Sr$ values were beyond the upper limit of the global calibration curve of McArthur et al. (2001) (marked with asterisk * in Table 2). In this study, four samples were analyzed from the same shallow boring and at the same level on different benthic foraminifera species (5.1/5.2; 65.5 m).

Like previous studies, three Sr ratios are higher than the upper limit with numerical age zero (Appendix A). One Sr age (150 ± 50 ka) (Table 2; Fig. 6d– marked with an empty triangle) is in-line with the previously proposed age which based on micropaleontological evidence and amino acid ratios suggested an Eemian interglacial age (Sejrup et al., 1989). To assign ages to the depth of seismic reflectors/boundary, Q1 to Q3, in the Quaternary sediment package in 16/1–8, the age-model equation (1) is used (Figs. 1b and 3). From this we have dated the following boundaries: Top Q1 = 1.73 ± 0.12 Ma; Top Q2 = 1.55 ± 0.07 Ma and Top Q3 = 1.30 ± 0.07 Ma. Moreover, using equation (1), the basal age of Q1 is ~2.59 ± 0.18 Ma at 612 m which is in-line with the previously assumed boundary between the Pliocene (Utsira Formation) and the Quaternary sediment package.

4.2. Amino acid racemization

Of the three species analyzed from 16/1–8 and 8903, *Elphidium excavatum* generally shows faster racemization (evidenced by higher D/L values) than the other species (Fig. 7). The D/L Asp value in *Elphidium excavatum* of MIS 2 radiocarbon-dated samples equals 0.30 ± 0.01, and other downcore samples range from 0.40 ± 0.02 to 0.85 ± 0.03 (Fig. 6). Demarchi and Collins (2014) suggested that the differences in the extent of racemization between taxa can be due to non-homogenous position of amino acids within the proteins. Distinctly low D/L values in *Cassidulina laevigata* at 387 m and 547 m in 16/1–8 are recorded in all amino acids (Fig. 7). At 387 m, the D/L Asp values in accepted subsamples after

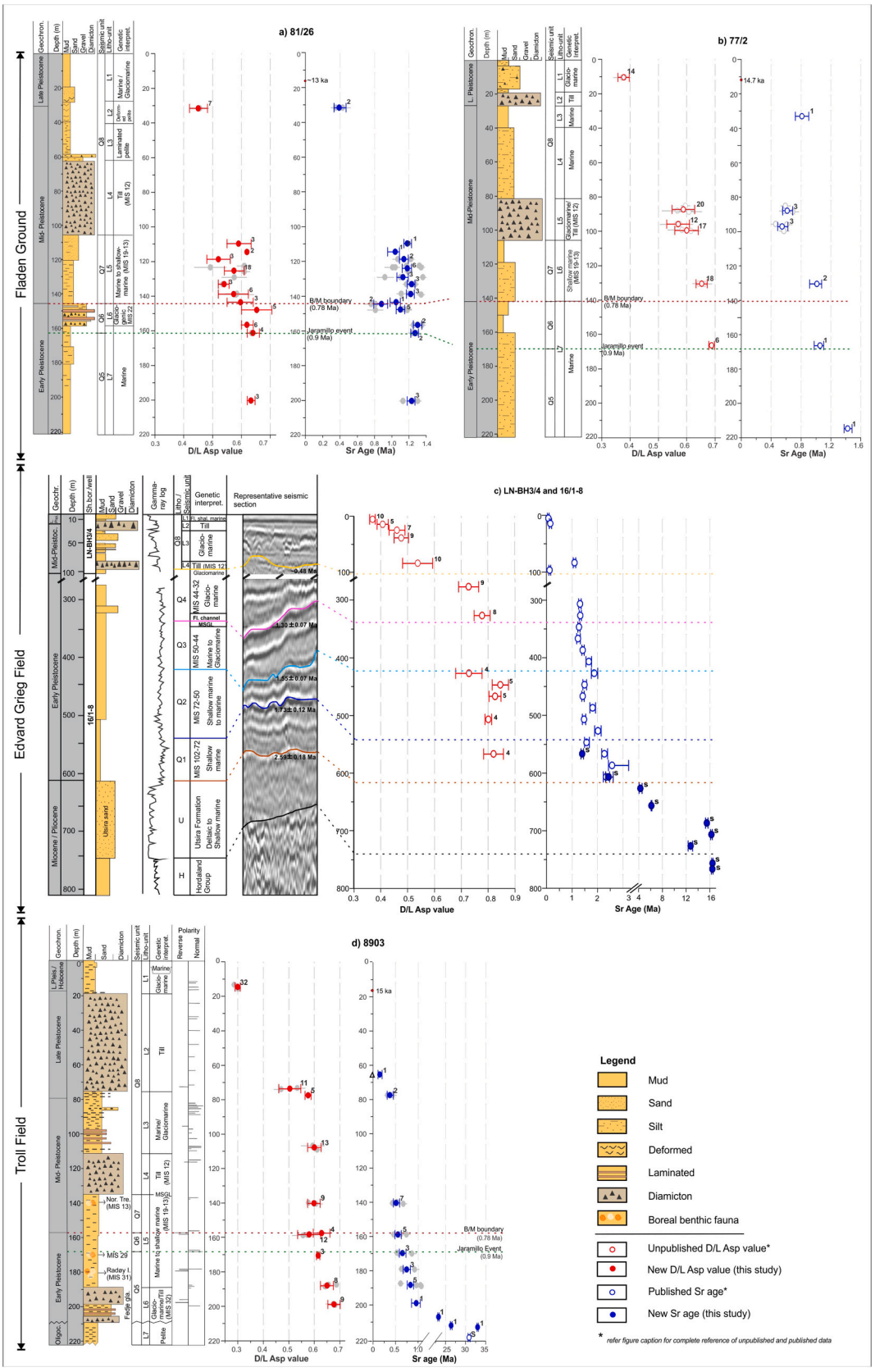

(caption on next page)

Fig. 6. Lithology, downcore distribution of D/L Asp in *Elphidium excavatum,* and downcore variation of Sr ages (in Ma) in shallow borings **a)** 81/26, **b)** 77/2, **c)** LN-BH3/4 & well 16/1–8 and **d)** 8903 are presented. Lithology logs for **a)** 81/26 and **d)** 8903 are modified after Sejrup et al. (1987; 1995); and **b)** 77/2 and **c)** LN-BH3/4 & 16/1–8 - lithology logs are modified after Reinardy et al. (2017, 2018). Empty circles show the unpublished D/L Asp values (red) and published Sr ages (blue) in **b)** and **c)** and the data is used from Reinardy et al. (2017; 2018); and one published Sr age in **d)** is from Sejrup et al. (1995). In all D/L Asp and Sr age panel, grey circle denotes the data used for averaging (*refer* Appendix A&C) and overlapping red & blue circles are averaged values presented in Table 2 and discussed in text. The numbers written next to the circle indicate the number of subsamples (D/L Asp) and samples (Sr ages) averaged. In lithological unit/seismic unit, boundaries of Quaternary seismic unit Q1 to Q3 are marked and a representative seismic section is presented; and four lithological units, L1 to L4, and its equivalent seismic unit, Q8, is marked in **c)** and Q5 to Q8 are Quaternary seismic units present in all shallow borings (Fig. 1b), **a), b)** and **d).** The ages assigned for each seismic unit are based on the age model from this study (*refer.* equation (1) and Fig. 3). In Sr age panels, the red dot with an age (in ka) on depth scale are calibrated radiocarbon ages from Sejrup et al. (1987) – 81/26, 77/2; Sejrup et al. (1994) – 8903, and empty triangle in **d)** is new Sr age from stratigraphically equivalent level in shallow boring 5.1/5.2 at 65 m. Note the difference in depth scale in the y-axis in **c)** and note the break in x-axis in Sr age panel in **c)** and **d).** Sr ages from shell fragments are marked with 'S' in **c)** and **d).** Red dotted lines = Brunhes/Matuyama (B/M) boundary and green dotted lines = Jaramillo paleomagnetic boundary. MIS = marine oxygen isotope stage; MSGL = mega-scale glacial lineation in **c)** and **d)** are after Reinardy et al. (2017) and Rise et al. (2004), respectively. In **c),** U = Utsira Formation; H = Hordaland Group; Fl. shal. marine = fluvial shallow marine and Fl. channel = fluvial Channel and in **d),** Nor. Tre. = Norwegian Trench Interglacial; Radøy I. = Radøy Interglacial; Fedje gla. = Fedje glaciation.

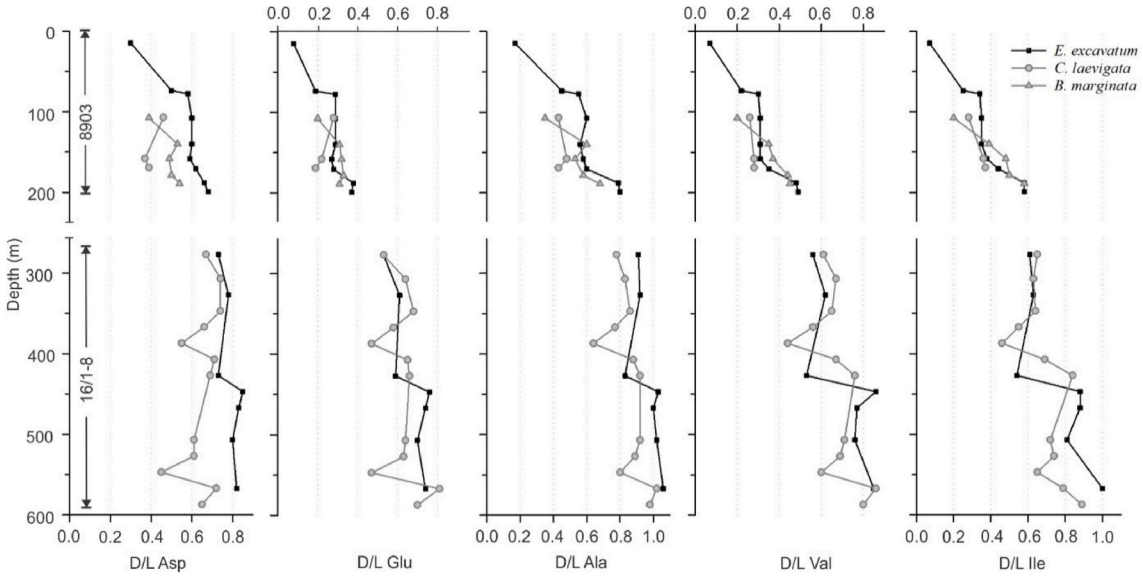

Fig. 7. Downcore distribution of five D/L values (Asp, Glu, Ala, Val, Ile) from three foraminifera species (*Elphidium excavatum, Cassidulina laevigata* and *Bulimina marginata*) in shallow boring 8903 (0–200 m) and two species (*Elphidium excavatum* and *Cassidulina laevigata*) in well 16/1–8 (270–600 m) are presented.

screening shows large uncertainty. D/L values vary from 0.47 to 0.69, possibly due to microbial activity, because a Sr age at 387 m (1.42 Ma) does not support caving of younger sediments as an explanation (Appendix C). However, at 547 m, a younger Sr age (1.5 Ma) indicate the possibility of caving of younger sediments while drilling the well, which corresponds to lower D/L Asp value. Because *Elphidium excavatum* seems to be less hampered by possible contamination and has good stratigraphic distribution, we concentrate on the results from this species.

To evaluate the local racemization pathways for the eight analyzed amino acids in *Elphidium excavatum*, D/L values are plotted against their respective Sr ages (Fig. 8). On understanding the pathway, we intended to use D/L Asp values for refining the chronology instead of establishing the kinetics of racemization process. Following the steps by Wehmiller et al. (2012) three regression plots (power, log, and linear) are drawn initially over D/L Asp to visualize the possible racemization pathways and understand the variability of D/L Asp with time (Fig. 8a). As the power regression curve seems to follow the data best, we use this in the following text to describe the local racemization pathway.

Some clusters of D/L Asp values do not fit the regression plots (Fig. 8a). These anomalous values are from specific levels in shallow boring 81/26 and well 16/1–8. The possible reasons for anomaly related to sediment deposition history are discussed later in section 5.2. These values are not included in the remaining regression plots (Fig. 8b–h). In general, the steeper parts of the curves have the best potential for age determination, whereas the lower gradient/levelling of the curve is associated with larger uncertainty. Relative to the other amino acids analyzed, the D/L Asp against the Sr age curve has a smaller uncertainty (Fig. 8b). The power regression curve of the relatively fast racemizing Asp starts flattening after approaching the ratio of 0.7 corresponding to ~2.0 Ma Sr age. However, the extrapolation of the power regression curve of D/L Asp can solve the age difference of samples up to 2.3 Ma but with higher uncertainty (Fig. 8b). D/L Glu racemizes relatively slowly and can resolve the chronology up to 2.5 Ma, but the older samples show higher uncertainty (Fig. 8c). Ala reaches equilibrium at ~2.0 Ma and is therefore not useful in deriving ages for the Early Pleistocene (Fig. 8d). Plots of D/L Val and D/L Ile against Sr ages show a similar trend, and both reach equilibrium around 2.2 Ma and 2 Ma, respectively (Fig. 8e and g).

D/L Asp and D/L Leu follow a similar path, but the uncertainty is higher in all D/L Leu *vs* Sr age correlation (Fig. 8h). Likewise, D/L Glu, D/L Ala, D/L Val, and D/L Ile follow almost the same trend, but as the older values show a relatively high uncertainty, these may not be suitable for dating the Quaternary sediments older than ~1.5 Ma. Therefore, the lower uncertainty of D/L Asp makes it more useful for geochronological purposes (Fig. 8i).

4.3. Uncertainties in ages

To clarify the uncertainty range in Sr isotope dating, McArthur et al. (2001) state that the conversion of Sr ratios to numerical ages does not

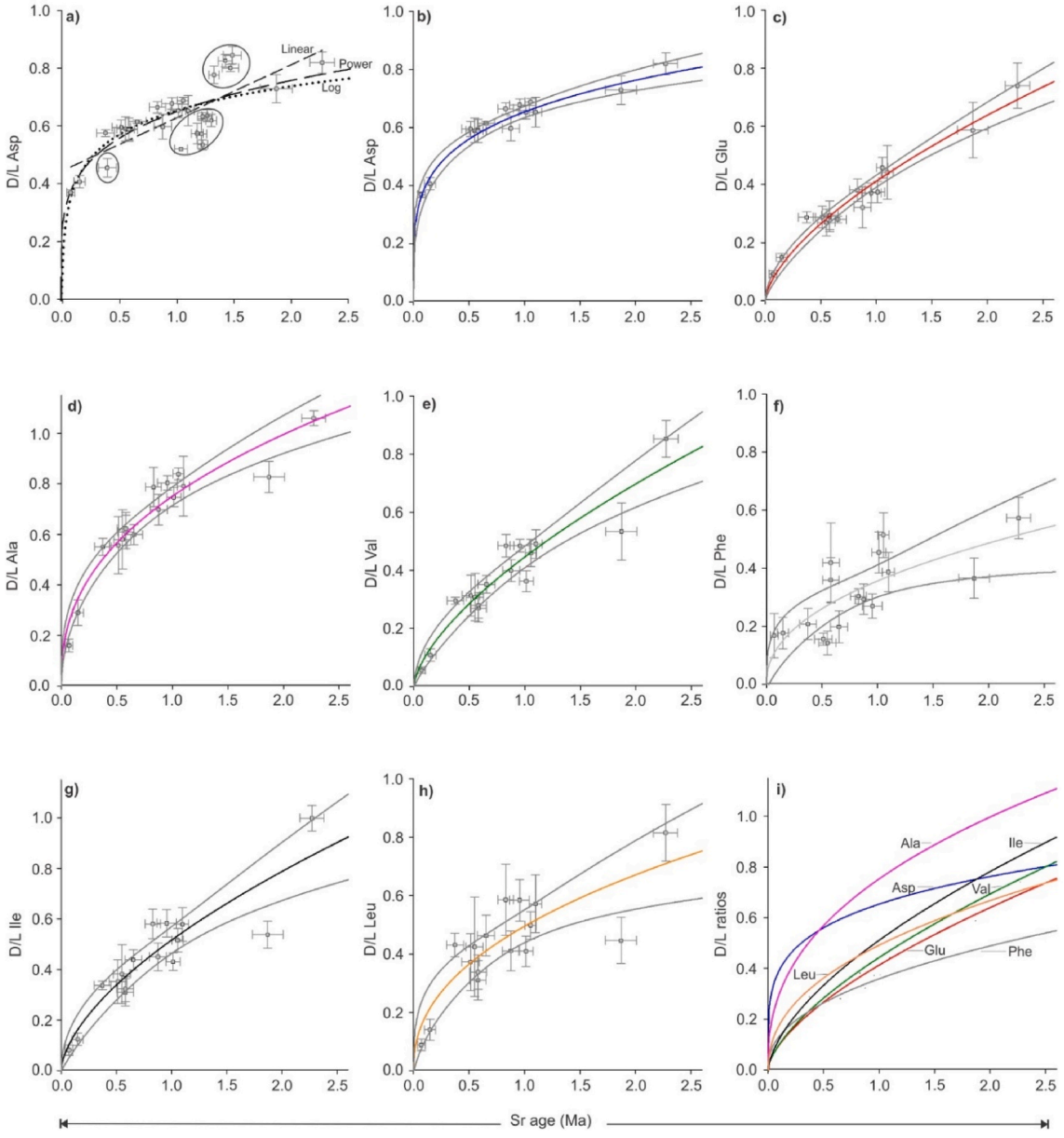

Fig. 8. D/L values vs Sr age for multiple amino acids. **a)** Three regression plots (power, log, and linear) are drawn over D/L values of aspartic acid (Asp). The power regression curve (long-dash) fits well and defines the pattern of racemization. The cluster of values which does not fit the regression curve is marked with a circle and not used in the remaining plots. These anomalous clusters represent the event of a riverine influx in 81/26 and reworking in 16/1–8. Refer to the discussion section in the main text for more details. **b to h)** Correlation between Sr ages and D/L values of aspartic acid (Asp), glutamic acid (Glu), alanine (Ala), valine (Val), phenylalanine (Phe), isoleucine (Ile), and leucine (Leu). The colored line is the power regression curve, and the envelope of the grey line is the 95% confidence interval. Bi-directional error bar shows the uncertainty limit of D/L Asp and Sr age **i)** Summary plot showing a kinetic model of seven amino acids.

give preferred ages; instead, it represents an age range with a 95% confidence interval. Moreover, the uncertainty in Sr ages includes the uncertainty of measurements of the sample Sr ratios and sample context. This point emphasizes the importance of considering the uncertainty of the ages in conclusions instead of building the discussion around a single age. A recent study by Eidvin et al. (2020) highlighted the risk of using Sr ages for the Quaternary sediments due to the lower gradient of the global Sr curve for the Pleistocene and the possibility of analyzing reworked fossils along the Norwegian coast related to glacial processes. Here, to interpret the Sr data, D/L Asp values and other supporting evidence are integrated to produce a reliable chronostratigraphic framework. Comparing Sr ages from ditch cutting samples in 16/1–8 and the possibly more dependable Sr ages from sidewall-core samples from the same seismic units of neighbouring well 16/1–4 (Eidvin et al., 2020) are encouraging and suggests insignificant influence from the drilling operation (caving). Uncertainties in the Sr dates have been estimated to range from 40 to 80 ka for samples younger than ~1.2 Ma from shallow borings (0–200 m) and 80–140 ka for samples older than 1.2 Ma from ditch cuttings (300 m and below in well 16/1–8). Likewise, within the Early Pleistocene sediment package, it is noted that Sr dates older than 1.5 Ma have a larger and asymmetric range of uncertainty from the calibration curve and age-depth model (equation (1)) (Fig. 3).

For the northern North Sea, D/L Asp in *Elphidium excavatum* has emerged as a valuable tool, both for samples from shallow borings (back to *c.* 1 Ma) and deeper ditch cutting material from the well 16/1–8. The calibration curve of D/L Asp values (equation (2)) can refine the Quaternary ages from the Late Pleistocene to part of the Early Pleistocene (~2 Ma) (Fig. 5b). Equation (2) based-ages (D/L Asp calibrated) suggest

uncertainty of 10–200 ka for the younger samples from shallow borings and larger uncertainty of 300–500 ka (3–10%) for older samples from 16/1–8 is estimated. The reason for a relatively larger uncertainty in D/L Asp calibrated ages for older samples is partly due to the flattening of the regression curve. We suggest that the D/L Asp calibrated age equation (2) could be helpful to date the Late to Mid Pleistocene sediments (50–781 ka), and to some extent for the upper part of Early Pleistocene sediments (781 ka to 1.1 Ma) compared to the lower part in Early Pleistocene (1.1–2.58 Ma) where uncertainty in estimated age is larger. Still, the most significant potential for the amino acid method must be as a relative dating method used in combination with other methods.

5. Discussion

5.1. Pre-quaternary depositional history

In the central North Sea, a Miocene age, *c.*16.4 Ma, is obtained from two Sr samples (757 and 767 m) of the Hordaland Group in well 16/1–8 (Fig. 6c). These Sr ages are within the age range (55–11 Ma) suggested for this Group based on biostratigraphy (Eidvin and Rundberg, 2007). Above the Hordaland Group (747 m) lies the Nordland Group, including the Utsira Formation-a 135 m thick sandy unit with low gamma-ray signal, and the overlying Pleistocene sediment package (Fig. 6c). Samples from the Utsira Formation represent a shallow marine environment (Eidvin et al., 2013) and five Sr ages are measured from this unit, of which the lower three ages are possibly reworked from the underlying unit. The remaining two ages in the Utsira Formation cover the timespan from Late Miocene to Early Pliocene, ~6–4 Ma (Fig. 6c). These ages are concurrent with the published chronology for the Utsira Formation based on foraminiferal biostratigraphy (Eidvin and Rundberg, 2001) and also with the Sr ages from the neighbouring (<5 km) side-wall core in 16/1–4 (Eidvin et al., 2020). The Sr age obtained from the top sample in the Utsira Formation (4.3 ± 0.2 Ma at 627 m) and lowermost sample in the Quaternary sediment package (2.4 ± 0.1 Ma at 607 m) indicate low sedimentation rates or a possible hiatus near the base-Quaternary boundary (Figs. 6c and 9). Lithologically, the presence of glauconite in sediment (Reinardy et al., 2017) also support this interpretation because glauconite authigenesis occurs in environments with low sedimentation rates (Dooley, 2006).

5.2. Early and Mid-Pleistocene events

Samples from the Quaternary seismic units Q1 to Q3 and part of Q4 (*after* Baig, 2018) have been examined in 16/1–8 between 607 m and 307 m (Figs. 1b and 6c). Ages to top of Q1–Q3 boundaries are calculated using the age-model equation (1): Top Q1 = 1.73 ± 0.12 Ma; Top Q2 = 1.55 ± 0.07 Ma and Top Q3 = 1.30 ± 0.07 Ma (Figs. 3 and 6c). Units Q5 to Q8 are studied in the shallow borings. The ages of top of Q4–Q8 units have been estimated based on paleomagnetic boundaries, Sr-dates, and the D/L Asp calibration-based equation (2) (Figs. 5 and 9). The estimated depositional age for the units is: Q4 = 1.3–1.1 Ma, Q5 = 1.1 Ma–990 ka, Q6 = 990–781 ka, Q7 = 781–480 ka and Q8 = 480 ka–recent.

5.2.1. Unit Q1 and Q2 (2.58 Ma to 1.5 Ma)

The results from D/L Asp values and Sr dates including a uniform lithology (from gamma logs) and seismic appearance suggest continuous sedimentation of seismic units Q1 and Q2 between 2.58 and 1.55 Ma in 16/1–8 (Fig. 6c) (Reinardy et al., 2017). However, during the transition from Q2 to Q3 at ~1.55 Ma, a shift in D/L Asp from 0.80 to 0.73 straddling the boundary, coincides with two consecutive somewhat older Sr ages of 1.87 and 1.66 Ma in 16/1–8 (427 and 407 m) (Fig. 6c). Comparably, an older Sr age of 1.75 Ma is also recorded in the side-wall core of 16/1–4, at the same stratigraphic level (Eidvin et al., 2020). The out of order Sr ages could be related to reworking, possibly by iceberg scouring as suggested during the Early Pleistocene (Rea et al., 2018; Løseth et al., 2020). The erratic values could also be the result of the influence of riverine influx diluting the Sr composition of seawater, lowering the Sr ratio, and giving older numerical ages. Riverine sediment input from the SE-NW into the central North Sea has been suggested by Ottesen et al. (2014). In addition, around 1.5 Ma, the Eridanos river system started collapsing, and the Rhine river system became a more prominent drainage pathway, supplying coarser sand and gravel to the North Sea eroded during severe glaciation of central Europe (Overeem et al., 2001; Cohen et al., 2014, 2017). Combining observations from these previous studies suggest that the study area was influenced by an ample sediment supply locally and freshwater influence from rivers around 1.5 Ma (~MIS 51).

5.2.2. Unit Q3 and Q4 (1.5 Ma to 1.1 Ma)

Based on the Sr age model (equation (1)), an age of 1.5–1.3 Ma (MIS 51–42) is suggested for Q3 in 16/1–8 (Figs. 3 and 6c). Reinardy et al. (2017) identified possible mega-scale glacial lineation (MSGL) close to the top of Q3 and glacially abraded granitic and volcanic material at the corresponding level in 16/1–8 (Fig. 6c). Using equation (1), we estimated this layer was deposited around 1.36 ± 0.07 Ma during *c.* MIS 48-44 and possibly is evidence of early extension of grounded ice to the central North Sea (Figs. 3, 6c and 9). Sediment samples up to the top of unit Q4 and the units above were not retrieved in 16/1–8; however, equation (2) derived age for the uppermost sample in Q4 (277 m; D/L Asp 0.727) is 1.29 ± 0.32 Ma (Fig. 5). Concurrently, the sediments above the angular unconformity in the Norwegian Channel are dated to around ~1.1 Ma (~MIS 32) in 8903, corresponding to the unconformity reflector at the top of unit Q4, suggesting that the basin-wide glaciation and erosion possibly occurred between 1.2 and 1.1 Ma (Figs. 1c, 6d and 9). In previous studies from the central part of northern North Sea, the interpreted age for possibly the same seismic reflector varies from 1.8 Ma (Buckley, 2012) to 800–400 ka (Ottesen et al., 2014). Reinardy et al. (2017) indicated that multiple glacial advances of grounded ice could have formed this horizon and, the extension of the ice sheet and erosion resulted in a regional unconformity.

5.2.3. Unit Q5 and Q6 (1.1 Ma to 781 ka)

In the Norwegian Channel, immediately above the regional unconformity, the glaciomarine/till unit-L6 in 8903, representing the Fedje glaciation, was suggested to correspond to the oldest evidence of the Fennoscandian Ice Sheet expansion into the North Sea (Sejrup et al., 1995) (Figs. 1b and 6d). A Sr age ranging from 0.85 to 1.04 Ma at 199 m, within unit-L6, gives an approximate numerical age of Fedje glaciation (Table 2). Moreover, in unit-L5, above the Fedje till, mean of five new Sr ages, 0.92 ± 0.11 Ma at 188.3 m, generally supports an age close to ~1.1 Ma ± 0.01, as suggested by Sejrup et al. (1995) (Table 2). Following this possible MIS 36-32 glaciation, the presence of Atlantic Water at the 8903 site was inferred from sub-polar planktic species and boreal benthic foraminiferal species (~180 m), and this event was named the Radøy Interglacial (Sejrup et al., 1995) (Fig. 6d). The foraminifera assemblage of sub-polar and boreal species suggests that the Radøy Interglacial possibly corresponds to a relatively warm interglacial. The Sr age corresponding to 180 m (0.67–0.83 Ma) suggest that the Radøy interglacial may possibly related to MIS 29 warming. However, based on the position of two paleomagnetic boundaries above and because MIS 31 was relatively warmer than MIS 29, we propose an age corresponding to MIS 31 (1.07 ± 0.01 Ma) for the Radøy Interglacial. Previous studies denote MIS 31 as one of the 'super interglacials' due to extremely warm conditions and suitability as an analogue for future warming (DeConto et al., 2012; Melles et al., 2012). Scherer et al. (2008) presented that the increase in summer insolation in the Southern Hemisphere during 1.08 Ma led to melting of Northern Hemisphere Ice Sheet and sea-level rise during 1.07 Ma; moreover, de Wet et al. (2016) recorded this event in the terrestrial Arctic. A later increase in boreal benthic species at 170 m, however, lower than foraminifera abundance at 180 m (MIS 31) may represent a relatively mild MIS 29 interglacial

(1.02 ± 0.008 Ma) (Fig. 6d). The transition from Q5 to Q6 occur close to the Jaramillo paleomagnetic boundary in the shallow borings 81/26, 77/2 and 8903. In the Fladen area, till (unit-L6) is deposited above the Jaramillo boundary in shallow boring 81/26. Considering its position between the Jaramillo (~0.99 Ma) and the B/M boundary (~0.78 Ma), we assign L6 to the MIS 22 glaciation, which occurred around 900 ka (Fig. 6d). Several studies suggest that this glacial stage represents a significant glaciation in NW Europe (*e.g.,* Clark et al., 2006; Elderfield et al., 2012; Rohling et al., 2014).

5.2.4. Unit Q7 – 781 to 480 ka

The B/M paleomagnetic boundary coincides with the boundary between seismic unit Q6 to Q7 in the Fladen and the Troll borings (Fig. 6a, b and 6d). In the Fladen shallow boring 81/26, average of two D/L Asp values close to B/M boundary equals ~0.65 within uncertainty limits (Fig. 6a). A rapid shift in the D/L Asp values at this level indicates the non-depositional or an erosional phase during the transition from the Early to Mid-Pleistocene (Fig. 6a). A similar shift was also recorded earlier in A/I values at the B/M boundary in 81/26 (Sejrup et al., 1987). Peaks of boreal benthic foraminifera, *Bulimina marginata,* and *Trifarina fluens* were recorded at this level, suggesting interglacial conditions and the Atlantic Water influence (Feyling-Hanssen, 1964; Sejrup et al., 1987). Likewise in 77/2, the first available D/L Asp value above the B/M boundary at 130.5 m is ~0.65 (Fig. 6b). In 8903, D/L Asp values at the B/M boundary overlaps with ~0.65 within uncertainty limit, however an inverse D/L Asp value of 0.56 at 158.8 m could be due to environmental factors (e.g., influence of Atlantic Water) or age of the fossil. We suggest an age of *c.* 781 ka, possibly reflecting MIS 19 for this interglacial stage. The older Sr ages (~1.2 Ma) above the B/M boundary in 81/26 (Fig. 6a) may be explained by the strong influence of river drainage resulting in diluting the Sr ratios with freshwater input. In the Troll boring 8903, a sudden abundance of subpolar planktic assemblages and boreal benthic species were observed in unit-L5 at *c.* 140 m and referred to as Norwegian Trench Interglacial (Sejrup et al., 1995). The D/L Asp value for this interglacial event is 0.60 ± 0.026 (Fig. 6d). Based on D/L Asp calibrated age (~511 ka) and the Sr age (~590–470 ka), we suggest an MIS 13 age (533–478 ka) for the Norwegian Trench Interglacial (Figs. 6d and 9). Above this interglacial, till unit-L4 was deposited and similar D/L Asp value of ~0.60 was recorded above the till, indicating the possibility of glaciotectonics and/or deposition of reworked material or the lack of temporal resolution. Similarly, in the Fladen area, a similar D/L Asp value (~0.60 ± 0.04) is recorded in 81/26 at 143.5 m in unit-L5 and corresponds to reworked Sr age of 1.05 Ma, and in 77/2, D/L Asp value of ~0.60 at 99.5 m within till unit-L5 also indicates the presence of reworked samples (Fig. 6a and b; Table 2). However, in the top 35 m of sediment in unit-L5, the abundance of boreal fauna and molluscs represents a shallow depositional environment (Sejrup et al., 1987), suggesting relatively warm conditions which possibly resulted in increased riverine input in Fladen area, influencing the Sr ratios (Fig. 6a and b). Although MIS 13 was recorded as relatively colder interglacial than other younger interglacials of the Mid-Pleistocene in Antarctica (Jouzel et al., 2007) and mid-latitude North-Atlantic (Voelker et al., 2010), other studies indicate MIS 13 was associated with vegetation abundance and reduced ice sheet conditions in Greenland (de Vernal and Hillaire-Marcel, 2008) and lack of extensive mountain glaciation in the continental Siberia (Prokopenko et al., 2002).

5.2.5. Unit Q8 (< 480 ka)

The oldest diamictons, interpreted as till units above the B/M boundary, has been suggested here to represent MIS 12 in the four shallow borings (81/26-L4; 77/2-L5; LN-BH3/4-L4, and 8903-L4 – Fig. 6). Evidence from 3D-seismic indicates the presence of MSGL at the base of till unit-L4 in the Norwegian Channel (Rise et al., 2004) (Fig. 6d). In the Troll shallow boring 8903, D/L Asp values (0.58 ± 0.012) and a Sr age (450–310 ka) is measured in the sample above the till unit-L4, whereas in 77/2 (L5) and LN-BH3/4 (L4) several D/L Asp values were obtained from foraminifera incorporated within till units (Fig. 6b, c and 6d). The Sr ages obtained from unit-L5 in 77/2 range from 690 to 460 ka (Fig. 6b). Since the D/L Asp values and Sr ages above and below the till unit are sparse; thus, to identify the age of the 'till', we considered the youngest Sr age out of three Sr ages within the till unit (460 ± 60 ka; 96 m – Appendix A) and the lowest D/L Asp value (0.59 ± 0.04; 95.8 m – Table 2) obtained within the till in 77/2 as the closest representative age or possibly a maximum age boundary of till deposition. Additionally, this combination of the lowest D/L Asp value and Sr age also matches well with the single D/L Asp value (0.59 ± 0.024), obtained above the till unit-L4 in 8903, where a comparable D/L Asp calibrated age (462 ka – equation (2)) is estimated, thereby validating this approach to identify the age (Figs. 5 and 6d). Thus, we propose that these till units may partly represent an extensive glacial event during MIS 12 (~478–424 ka); however, some of them may represent younger glacial stages as anticipated by Sejrup and Knudsen (1999) and Reinardy et al. (2018). Likewise, earlier studies also suggest large expansion of British Ice Sheet in the North Sea region during MIS 12 based on the evidence of tills and glaciomarine deposit in the sedimentary record (Holmes, 1997; Carr, 2004; Lee et al., 2011).

5.3. Implications for the chronology of the North Sea

At the onset of the Quaternary, a period of low or no sedimentation at the base of the Quaternary succession is marked by a distinct down-lap seismic horizon towards the central North Sea (Baig, 2018) (Fig. 1c). In this study, the Sr ages indicate a period of no sedimentation or low sedimentation rates existed around the Pliocene-Pleistocene boundary (Figs. 6c and 9). Lamb et al. (2018) propose that two depo-centers were present during the deposition of sediments in the Early Pleistocene: one with high sedimentation rates in the southern North Sea and another with lower sedimentation rates in the northern North Sea between 2.58 and 2.53 Ma. The Early Pleistocene is much more compressed than previously envisaged and is a crucial factor when estimating the volume of the Quaternary sediment packages and determining the ages of glacial features observed on acoustic data (Baig, 2018).

Another key issue is the timing of the first grounded ice in the central North Sea, which is still unclear. Earlier, a wide range of ages were suggested from 1.8 Ma (Buckley, 2012) to 800–400 ka (Upper Regional Unconformity; Ottesen et al., 2014) for the bright seismic reflector mapped in these studies. In this study, the equivalent of this bright seismic reflector is the top of unit Q4, and the older sediment package below Q4 is truncated towards the east and west margin of the basin (Figs. 1c, 6c and 9). Buckley (2017) identified a sequence of MSGL (~1.1 Ma) and overlying fluvial/tunnel valley (~1 Ma) around this seismic horizon as evidence of the first ice sheet advance and decay. Concurrently, Reinardy et al. (2017) examined similar geomorphological features within unit Q3 and Q4, and using age model equation (1), an age of 1.36 Ma is estimated for this feature and using equations in Appendix B, an uncertainty of ±70 ka is calculated. We infer that possibly the first ice sheet extended to the central North Sea around 1.36 ± 0.07 Ma during *c.* MIS 48-44, based on relatively greater erosional capacity resulting in a regional unconformity across the basin (Fig. 9). This is reflected by the dating of the oldest sediments above the unconformity in the Norwegian Channel to around 1.1 Ma (Sejrup et al., 1995). Moreover, the ages derived from top and bottom of this regional unconformity in the Fladen Ground (81/26, 77/2) and our new chronological information indicates that the major basin-wide glaciation occurred around 1.1 Ma. The Sr ages from the 16/1–8, LN-BH3/4 also suggest that this unconformity developed between 1.2 Ma and ~1 Ma (Figs. 6c and 9).

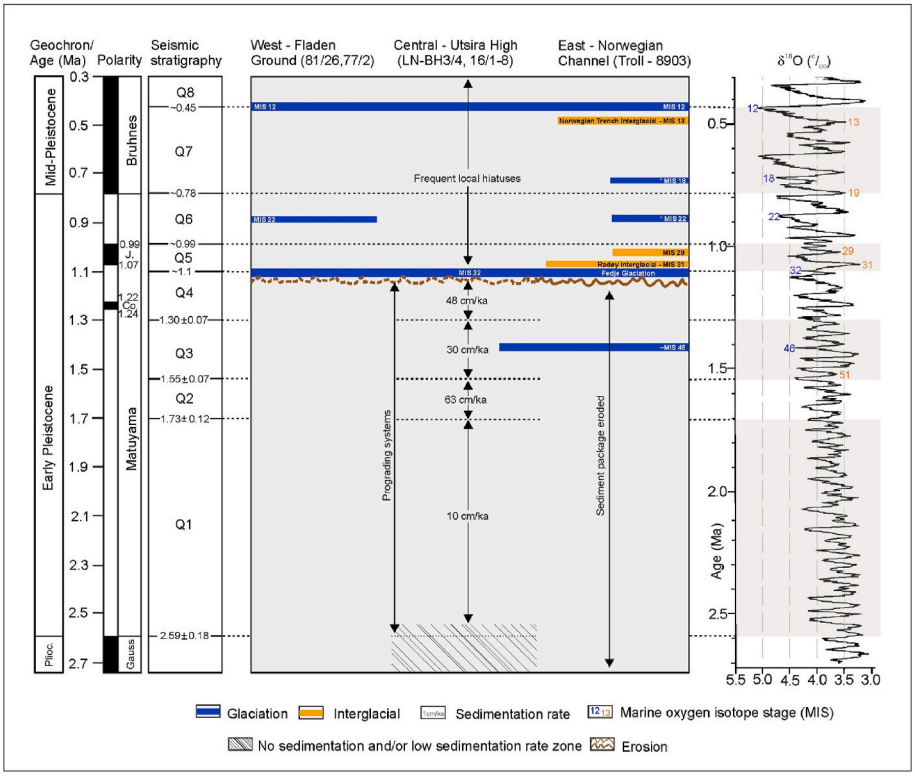

Fig. 9. Summary figure (not to scale) illustrating the geochronological results of the sediment package deposited in the northern North Sea during glacial-interglacial cycles of the Early and Mid-Pleistocene. Eight seismic units (Q1 to Q8) are dated, and sedimentation rates are estimated. The ages of Q1 to Q3 boundaries are based on the Sr age model with uncertainties (equation (1)) and ages of Q4 to Q8 based on D/L Asp calibration curve (equation (2)) and other supportive geochronological evidence (paleomagnetic boundary and radiocarbon age). Dashed brown line imply erosion within the same sediment package whereas full brown erosion line implies erosion of sediment package up to Oligocene in the Norwegian Channel. It was probably resulted from multiple glacial-interglacial events. In polarity panel, J = Jaramillo event; Co = Cobb Mountain event. Evidence of glaciation and marine oxygen isotope stage (MIS) marked with asterisk* in the Norwegian Channel are after Sejrup et al. (2003).

6. Conclusions

New amino acid racemization (reverse-phase chromatography) and Sr isotope dating of the Early to Mid-Pleistocene foraminifera samples from the four shallow borings (81/26, 77/2, LN-BH3/4, and 8903) and one well (16/1–8) in a transect across the northern North Sea, is presented.

D/L Asp value in benthic foraminifera species *Elphidium excavatum* is shown to be a promising tool for geochronological studies on the Quaternary sediments in the North Sea. An age model based on Sr ages for the Early Pleistocene sediments in well 16/1–8 from the central North Sea (equation (1)) allow for the dating of the Early and Mid-Pleistocene regional seismic units in the northern North Sea. A nearly consistent D/L Asp value (~0.65) at the B/M paleomagnetic boundary suggests a similar temperature history along the transect, which is crucial for using the amino acid method for correlation. Based on radiocarbon ages, paleomagnetic data, and Sr ages, a calibration curve for D/L Asp (equation (2)) is proposed. Furthermore, MIS correlations are made based on multiple lines of geochronological evidence. Quantifying the uncertainties associated with these assigned ages is challenging but are estimated to range from 10 to 70 ka. In addition, we have evaluated the implications of the assigned ages with respect to the available faunal data.

Based on the new and existing chronological data, the following conclusions are made:

- A rapid increase in sedimentation rates close to 1.5 Ma (~MIS 51) in the central North Sea may partly associated with sediment supply from rivers and partly reflect glacial ice extending from the Norwegian coast, possibly for the first time around ~1.36 Ma ± 0.07 during *c.* MIS 48-44 (or ~1.4 Ma corresponding to MIS 46) (Fig. 9).
- A major basin-wide glaciation dated to around 1.1 Ma (~MIS 32) is evidenced by massive erosion and a regional unconformity.
- Two interglacials with subpolar foraminiferal faunas recorded in the Norwegian Channel have been dated: the Radøy Interglacial suggested to be of MIS 31 age ('super-interglacial') and the Norwegian Trench Interglacial of MIS 13 age (Fig. 9).
- Till units identified in all investigated shallow borings across the basin at the same stratigraphic level may be partly represent an extensive MIS 12 glaciation.

To construct a stratigraphic framework, especially in regions with episodic sedimentation and reworking, integration of amino acid racemization and strontium isotope stratigraphy is a possible approach to obtain reliable chronologies.

Declaration of competing interest

The authors declare that they have no known competing financial interests or personal relationships that could have appeared to influence the work reported in this paper.

Acknowledgement

We acknowledge the Research Council of Norway for funding the REQUBE project through the Petromaks2 program (RCN:190748). Lundin Norway A/S is thanked for providing well cuttings and seismic data. Thanks to Vigdis Clausen-Hope for technical support and Yuval Ronen for performing Strontium Isotope analysis at the University of Bergen. We acknowledge Katherine Whitacre and Jordon Bright for guiding in AAR sample processing and carrying out the analysis at the Amino Acid Geochronology Laboratory, Northern Arizona University, Arizona, USA (National Science Foundation (NSF) 1855381). Thanks to Tor Eidvin (Norwegian Petroleum Directorate) for valuable discussions. We are especially grateful to two anonymous reviewers and the journal editor Kirsty Penkman for providing constructive comments and suggestions on the manuscript.

Appendix A

$^{87}Sr/^{86}Sr$ values are obtained from foraminifera in 81/26, 8903, 5.1/5.2, and from shell fragments in 16/1–8. Previously published foraminifera-based Sr ages from 77/2, LN-BH3/4, and 16/1–8 (Reinardy et al., 2017, 2018) are also shown here. Corrected $^{87}Sr/^{86}Sr$ values are converted to strontium (Sr) ages using the calibration curve by McArthur et al. (2001) and analytical error for strontium isotope analyses (2σ error) is included. Sr ages and depth are averaged and maximum (Max.), Mean and minimum (Min) ages are also calculated and grouped. Each group is demarcated by line. Sr ages in bold are excluded and not used in averaging. Ages marked with an asterisk (*) in 8903 and 5.1/5.2 are from Sejrup et al. (1995).

Sample ID	Depth (m)	Benthic foraminifera	Corrected $^{87}Sr/^{86}Sr$	2σ error	Min. age	Mean age (Ma)	Max. age	Avg. Min.	Avg. age (Ma)	Avg. Max.	Average depth
Fladen Ground - 81/26 (This study)											
8923	31.6	*Elphidium excavatum*	0.709162	0.000009	0.37	0.43	0.52	0.33	0.39	0.47	31.6
8924	31.6	*Elphidium excavatum*	0.709164	0.000008	0.30	0.35	0.42				
8925	109.7	*Elphidium* spp.	0.709127	0.000008	1.14	1.18	1.23	1.14	1.18	1.23	109.7
8926	114.5	*Elphidium* spp.	0.709138	0.000009	0.95	1.04	1.09	0.95	1.04	1.09	114.5
8927	118.7	*Elphidium excavatum*	0.709124	0.000010	1.17	1.22	1.26	1.09	1.14	1.19	118.7
8928	118.7	*Elphidium excavatum*	0.709136	0.000009	1.01	1.07	1.12				
8929	122.5	*Elphidium excavatum*	0.709128	0.000008	1.13	1.17	1.22	1.12	1.18	1.23	123.9
8930	122.5	*Elphidium excavatum*	0.709115	0.000008	1.28	1.32	1.37				
8951	123.4	*Elphidium excavatum*	0.709114	0.000009	1.29	1.34	1.38				
8952	123.4	*Elphidium excavatum*	0.709138	0.000009	0.95	1.04	1.09				
8953	123.4	*Elphidium excavatum*	0.709139	0.000009	0.92	1.01	1.08				
8954	125.9	*Elphidium excavatum*	0.709126	0.000009	1.15	1.19	1.24				
8955	129.1	*Elphidium excavatum*	0.709112	0.000008	1.31	1.36	1.41	1.06	1.13	1.19	129.1
8956	129.1	*Elphidium excavatum*	0.709134	0.000009	1.05	1.10	1.14				
8957	129.1	*Elphidium excavatum*	0.709142	0.000007	0.83	0.92	1.02				
8958	133.1	*Elphidium excavatum*	0.709128	0.000009	1.13	1.17	1.22	1.18	1.23	1.27	133.1
8959	133.1	*Elphidium excavatum*	0.709120	0.000009	1.22	1.27	1.31				
8960	133.1	*Elphidium excavatum*	0.709122	0.000009	1.19	1.24	1.29				
8931	138.6	*Elphidium excavatum*	0.709133	0.000009	1.06	1.11	1.15	1.17	1.22	1.26	138.8
8932	138.6	*Cassidulina laevigata*	0.709125	0.000009	1.16	1.20	1.25				
8933	139.1	*Elphidium excavatum*	0.709114	0.000008	1.29	1.34	1.38				
8934	143.5	*Elphidium excavatum*	0.709137	0.000009	0.98	1.05	1.10	0.98	1.05	1.10	143.5
8935	144.5	*Uvigerina peregrina*	0.709148	0.000009	0.68	0.76	0.85	0.70	0.79	0.88	144.5
8936	144.5	*Uvigerina peregrina*	0.709146	0.000009	0.72	0.81	0.90				
8937	147.5	*Uvigerina peregrina*	0.709131	0.000009	1.09	1.13	1.18	1.05	1.10	1.15	147.7
8938	147.5	*Uvigerina peregrina*	0.709127	0.000010	1.14	1.18	1.23				
8939	148.0	*Elphidium excavatum*	0.709127	0.000008	1.14	1.18	1.23				
8940	148.0	*Elphidium excavatum*	0.709146	0.000009	0.72	0.81	0.90				
8941	148.0	*Elphidium* spp.	0.709127	0.000009	1.14	1.18	1.23				
8942	156.6	*Elphidium excavatum*	0.709113	0.000008	1.30	1.35	1.39	1.25	1.30	1.35	156.6
8943	156.6	*Elphidium excavatum*	0.709121	0.000009	1.21	1.25	1.30				
8944	161.3	*Elphidium excavatum*	0.709097	0.000009	**1.53**	**1.63**	**1.74**	1.22	1.27	1.31	161.3
8945	161.3	*Elphidium excavatum*	0.709122	0.000008	1.19	1.24	1.29				

(*continued on next page*)

(*continued*)

Sample ID	Depth (m)	Benthic foraminifera	Corrected $^{87}Sr/^{86}Sr$	2σ error	Min. age	Mean age (Ma)	Max. age	Avg. Min.	Avg. age (Ma)	Avg. Max.	Average depth
8946	161.3	*Elphidium excavatum*	0.709118	0.000008	1.24	1.29	1.33				
8947	200.3	*Elphidium excavatum*	0.709131	0.000009	1.09	1.13	1.18	1.18	1.23	1.27	200.3
8948	200.3	*Elphidium excavatum*	0.709147	0.000008	**0.70**	**0.79**	**0.88**				
8949	200.3	*Cassidulina laevigata*	0.709117	0.000009	1.25	1.30	1.34				
8950	200.3	*Cassidulina laevigata*	0.709122	0.000008	1.19	1.24	1.29				
Fladen Ground - 77/2 (Reinardy et al., 2018)											
7576	10.6	*Elphidium excavatum*	0.709215	0.000009		**0.00**					
7577	33.0	*Elphidium excavatum*	0.709164	0.000007	0.30	0.35	0.42	0.30	0.35	0.42	33.2
7578	33.4	*Elphidium excavatum*	0.709200	0.000009		**0.00**					
7579	85.1	*Elphidium excavatum*	0.709165	0.000010	0.26	0.32	0.38	0.46	0.53	0.60	87.7
7580	88.1	*Elphidium excavatum*	0.709157	0.000008	0.51	0.57	0.64				
7581	88.6	*Elphidium excavatum*	0.709151	0.000009	0.62	0.69	0.77				
7582	88.9	*Elphidium excavatum*	0.709135	0.000009	**1.03**	**1.08**	**1.13**				
7583	95.7	*Elphidium excavatum*	0.709161	0.000009	0.40	0.46	0.56	0.49	0.55	0.62	97.2
7584	96.0	*Elphidium excavatum*	0.709155	0.000008	0.55	0.61	0.68				
7585	99.8	*Elphidium excavatum*	0.709157	0.000009	0.51	0.57	0.64				
7586	130.4	*Elphidium excavatum*	0.709139	0.000009	0.92	1.01	1.08	0.92	1.01	1.08	130.5
7587	130.7	*Elphidium excavatum*	0.709139	0.000010	0.92	1.01	1.08				
7588	157.1	*Elphidium excavatum*	0.709149	0.000007	0.66	0.74	0.82	0.66	0.74	0.82	157.1
7589	166.4	*Elphidium excavatum*	0.709137	0.000007	0.98	1.05	1.10	0.98	1.05	1.10	166.4
7590	214.7	*Elphidium excavatum*	0.709107	0.000009	1.38	1.42	1.48	1.38	1.42	1.48	214.7
Edvard Grieg - LN-BH3/4 (Reinardy et al., 2017)											
7591	14.5	*Elphidium excavatum*	0.709170	0.000009	0.11	0.15	0.20	0.11	0.15	0.20	14.5
7592	25.0	*Elphidium excavatum*	0.709175	0.000008		**0.00**					
7593	51.4	*Elphidium excavatum*	0.709173	0.000009	0.03	0.07	0.11	0.03	0.07	0.11	5.1
7594	84.0	*Elphidium excavatum*	0.709134	0.000009	**1.05**	**1.10**	**1.14**				
7595	97.0	*Elphidium excavatum*	0.709171	0.000012	**0.09**	**0.12**	**0.17**				
Edvard Grieg - 16/1–8 (Foraminifera Sr age - Reinardy et al., 2017 & Shell fragments Sr age - This study)											
7755	307	*Cassidulina laevigata*	0.709116	0.000008	1.26	1.31	1.36				
7756	327	*Cassidulina laevigata*	0.709115	0.000009	1.28	1.32	1.37				
7757	347	*Elphidium excavatum*	0.709120	0.000008	1.22	1.27	1.31				
7758	367	*Elphidium excavatum*	0.709123	0.000009	1.18	1.23	1.28				
7759	387	*Elphidium excavatum*	0.709107	0.000008	1.38	1.42	1.48				
7760	407	*Cassidulina laevigata*	0.709096	0.000009	**1.55**	**1.66**	**1.77**				
7761	427	*Elphidium excavatum*	0.709089	0.000009	**1.76**	**1.87**	**2.01**				

(*continued on next page*)

(*continued*)

Sample ID	Depth (m)	Benthic foraminifera	Corrected $^{87}Sr/^{86}Sr$	2σ error	Min. age	Mean age (Ma)	Max. age	Avg. Min.	Avg. age (Ma)	Avg. Max.	Average depth
7762	447	*Cassidulina laevigata*	0.709103	0.000008	1.43	1.49	1.57				
7763	467	*Cassidulina laevigata*	0.709107	0.000008	1.38	1.42	1.48				
7764	487	*Cassidulina laevigata*	0.709091	0.000008	1.70	1.81	1.92				
7765	507	*Cassidulina laevigata*	0.709104	0.000008	**1.41**	**1.47**	**1.54**				
7766	527	*Cassidulina laevigata*	0.709085	0.000008	1.89	2.02	2.14				
7767	547	*Cassidulina laevigata*	0.709099	0.000008	**1.49**	**1.57**	**1.68**				
7768	567	*Melonis barleeanus*	0.709077	0.000009	2.17	2.27	2.40				
9121	567	Shell fragments	0.709109		**1.35**	**1.40**	**1.45**				
7769	587	*Melonis barleeanus*	0.709069	0.000008	2.43	2.57	3.22				
7770	607	*Melonis barleeanus*	0.709075	0.000008	2.23	2.34	2.47				
9122	607	Shell fragments	0.709072		2.32	2.44	2.61				
9123	627	Shell fragments	0.709051		4.04	4.30	4.56				
9124	657	Shell fragments	0.708975		6.09	6.14	6.22				
9125	687	Shell fragments	0.708766		**15.26**	**15.48**	**15.67**				
9126	707	Shell fragments	0.708733		**16.09**	**16.25**	**16.39**				
9127	727	Shell fragments	0.708822		**12.35**	**12.76**	**13.09**				
9128	757	Shell fragments	0.708722		16.31	16.44	16.56				
9129	767	Shell fragments	0.708724		16.27	16.41	16.53				
Troll - 5.1/5.2 (This study & Sejrup et al., 1995*)											
8877	65.5	*Bulimina marginata*	0.709178	0.000009		**0.00**					
8878	65.5	*Uvigerina peregrina*	0.709191	0.000009		**0.00**					
8879	65.5	*Cassidulina laevigata*	0.709170	0.000007	0.11	0.15	0.20	0.11	0.15	0.20	65.5
8880	65.5	*Melonis barleanus*	0.709158	0.000009	**0.49**	**0.55**	**0.61**				
	65.5*	*Bulimina marginata*	0.709223	0.000019		**0.00***					
	65.5*	*Elphidium excavatum*	0.709199	0.000018		**0.00***					
Troll - 8903 (This study & Sejrup et al., 1995*)											
8870	74.0	*Cassidulina reniforme*	0.709179	0.000009		**0.00**					
8881	77.5	*Bulimina marginata*	0.709165	0.000008	0.26	0.32	0.38	0.31	0.37	0.45	77.5
8882	77.5	*Elphidium excavatum*	0.709162	0.000008	0.37	0.43	0.52				
8884	106.8	*Bulimina marginata*	0.709183	0.000009		**0.00**					
8885	106.8	*Elphidium excavatum*	0.709191	0.000008		**0.00**					
8883	107.5	*Bulimina marginata*	0.709198	0.000009		**0.00**					
8886	109.1	*Elphidium excavatum*	0.709183	0.000009		**0.00**					
8887	109.1	*Elphidium* spp.	0.709170	0.000009	**0.11**	**0.15**	**0.20**				
8888	109.3	*Elphidium excavatum*	0.709192	0.000009		**0.00**					
	138.4*	*Bulimina marginata*	0.709075	0.000015		**2.37***					
	138.4*	*Elphidium excavatum*	0.709097	0.000010		**1.62***					
8891	139.9	*Elphidium excavatum*	0.709169	0.000009	**0.13**	**0.18**	**0.23**	0.45	0.51	0.59	140.4
8892	139.9	*Bulimina marginata*	0.709159	0.000009	0.46	0.53	0.59				
8893	139.9	*Bolivina alata*	0.709171	0.000009	**0.09**	**0.12**	**0.17**				
8894	139.9	*Islandiella norcrossi*	0.709174	0.000010		**0.04**	**0.08**				
8895	140.2	*Elphidium excavatum*	0.709158	0.000009	0.49	0.55	0.61				
8896	140.2	*Elphidium excavatum*	0.709159	0.000008	0.46	0.53	0.59				

(*continued on next page*)

(*continued*)

Sample ID	Depth (m)	Benthic foraminifera	Corrected $^{87}Sr/^{86}Sr$	2σ error	Min. age	Mean age (Ma)	Max. age	Avg. Min.	Avg. age (Ma)	Avg. Max.	Average depth
8897	140.2	*Bulimina marginata*	0.709176	0.000009		**0.00**					
8898	140.5	*Elphidium excavatum*	0.709162	0.000008	0.37	0.43	0.52				
8899	140.5	*Islandiella norcrossi*	0.709162	0.000007	0.37	0.43	0.52				
8900	140.5	*Bulimina marginata*	0.709161	0.000009	0.40	0.46	0.56				
8901	140.5	*Cassidulina laevigata*	0.709175	0.000011		**0.00**					
8902	140.9	*Bulimina marginata*	0.709152	0.000009	0.60	0.67	0.75				
8871	158.9	*Bulimina marginata*	0.709155	0.000009	0.55	0.61	0.68	0.53	0.60	0.68	158.9
8872	158.9	*Bulimina marginata*	0.709149	0.000009	0.66	0.74	0.82				
8873	158.9	*Elphidium excavatum*	0.709161	0.000009	0.40	0.46	0.56				
8874	158.9	*Elphidium excavatum*	0.709164	0.000009	**0.30**	**0.35**	**0.42**				
8875	158.9	*Cassidulina laevigata*	0.709156	0.000009	0.53	0.59	0.66				
8876	158.9	*Cassidulina laevigata*	0.709189	0.000010		**0.00**					
8916	169.5	*Bulimina marginata*	0.709159	0.000008	0.46	0.53	0.59	0.58	0.65	0.73	169.8
8917	169.5	*Melonis barleeanus*	0.709174	0.000009		**0.04**	**0.08**				
	169.5*	*Bulimina marginata*	0.709046	0.000010		**4.64***					
	169.5*	*Elphidium excavatum*	0.709121	0.000020		**1.25***					
8918	170.0	*Bulimina marginata*	0.709157	0.000009	0.51	0.57	0.64				
8919	170.0	*Bulimina marginata*	0.709144	0.000009	0.78	0.86	0.96				
8920	170.6	*Bulimina marginata*	0.709179	0.000009		**0.00**					
8890	178.6	*Bulimina marginata*	0.709167	0.000008	**0.19**	**0.25**	**0.31**	0.67	0.75	0.83	179.3
8889	179.0	*Bulimina marginata*	0.709154	0.000008	0.57	0.63	0.70				
8921	179.3	*Melonis barleeanus*	0.709142	0.000008	0.83	0.92	1.02				
8922	179.5	*Uvigerina marginata*	0.709151	0.000009	0.62	0.69	0.77				
8913	187.5	*Elphidium excavatum*	0.709155	0.000009	0.55	0.61	0.68	0.85	0.92	0.99	188.3
8914	187.5	*Bulimina marginata*	0.709161	0.000009	**0.40**	**0.46**	**0.56**				
8915	187.5	*Elphidium* spp.	0.709164	0.000009	**0.30**	**0.35**	**0.42**				
8903	188.5	*Elphidium excavatum*	0.709137	0.000008	0.98	1.05	1.10				
8904	188.5	*Bulimina marginata*	0.709141	0.000009	0.85	0.96	1.04				
8905	188.5	*Cassidulina laevigata*	0.709169	0.000010	**0.13**	**0.18**	**0.23**				
8906	189.0	*Bulimina marginata*	0.709136	0.000008	1.01	1.07	1.12				
8907	198.7	*Elphidium excavatum*	0.709162	0.000009	**0.37**	**0.43**	**0.52**	0.85	0.96	1.04	199.0
8908	198.7	*Elphidium* spp.	0.709141	0.000009	0.85	0.96	1.04				
8909	199.2	*Elphidium excavatum*	0.709158	0.000008	**0.49**	**0.55**	**0.61**				
	201.2*	*Elphidium excavatum*	0.708991	0.000027	**5.90**	**5.95***	**5.99**	5.9	5.95	5.99	201.2
8910	207.0	Mixed Benthic	0.708279	0.000009	**23.06**	**23.25**	**23.42**	23.06	23.25	23.42	207.0
8911	212.0	Mixed Benthic	0.708121	0.000009	26.18	26.41	26.65	26.18	26.41	26.65	212.0
8912	213.0	Mixed Benthic	0.707851	0.000008	32.85	33.00	33.18	32.85	33.00	33.18	213.0
	219.0*	Alabamina sp.	0.707951	0.000019	30.63	30.87*	31.1	30.63	30.87	31.12	219.0

Appendix B

Coefficients of fourth-order polynomial equations through LINEST function (Morrison, 2015) to calculate the age from equation (1) and, minimum and maximum range of age-depth model curve given in equation (1) and presented in Fig. 5.

Fourth order Polynomial Equation: $A = a4d^4 + a3d^3 + a2d^2 + a1d + a0$					
where, A = age in million years (Ma), d = depth in meters below sea level					
t (mean)					
Coefficients	a4	a3	a2	a1	a0
	0.000000001168	−0.000002015601	0.001285436544	−0.356465307704	37.522222589829
R2	0.69				
t (min)					
Coefficients	a4	a3	a2	a1	a0
	0.000000001190	−0.000002058482	0.001315553409	−0.365902150988	38.582747712513
R2	0.68				
t (max)					
Coefficients	a4	a3	a2	a1	a0
	0.000000000889	−0.000001482406	0.000911906902	−0.242730090679	24.873544122010
R2	0.63				

Appendix C and D. Supplementary data

Supplementary data to this article can be found online at https://doi.org/10.1016/j.quageo.2022.101336.

References

Baig, I., 2018. Burial and Thermal Histories of Sediments in the Southwestern Barents Sea and North Sea Areas: Evidence from Integrated Compaction, Thermal Maturity and Seismic Stratigraphic Analyses. Department of Geosciences. University of Oslo, pp. 1–194.

Brigham-Grette, J., Sejrup, H.P., 1985. Stratigraphic applications of amino acid geochronology in North Sea sediments. Geol. Soc. Am. Abstr. Progr. 17, 531.

Buckley, F.A., 2012. An early Pleistocene grounded ice sheet in the central North sea. Geol. Soc. London, Special Publ. 368, 185.

Buckley, F.A., 2017. A glaciogenic sequence from the early Pleistocene of the central North sea. J. Quat. Sci. 32, 145–168.

Carr, S.J., 2004. the North sea basin. In: Ehlers, J., Gibbard, P.L. (Eds.), Quaternary Glaciations—Extent and Chronology,Part I: Europe. Elsevier, Amsterdam, pp. 261–270.

Clark, P.U., Archer, D., Pollard, D., Blum, J.D., Rial, J.A., Brovkin, V., Mix, A.C., Pisias, N. G., Roy, M., 2006. The middle Pleistocene transition: characteristics, mechanisms, and implications for long-term changes in atmospheric pCO2. Quat. Sci. Rev. 25, 3150–3184.

Cohen, K.M., Gibbard, P.L., Weerts, H.J.T., 2014. North Sea palaeogeographical reconstructions for the last 1 Ma. Netherlands J. Geosci. -Geologie En Mijnbouw 93, 7–29.

Cohen, K.M., Westley, K., Erkens, G., Hijma, M.P., Weerts, H.J.T., 2017. the North sea. In: Flemming, N.C., Harff, J., Moura, D., Burgess, A., Bailey, G.N. (Eds.), Submerged Landscapes of the European Continental Shelf : Quaternary Paleoenvironments. John Wiley & Sons, Inc., Oxford, UK, pp. 147–186.

de Vernal, A., Hillaire-Marcel, C., 2008. Natural variability of Greenland climate, vegetation, and ice volume during the past million years. Science 320, 1622.

de Wet, G.A., Castañeda, I.S., DeConto, R.M., Brigham-Grette, J., 2016. A high-resolution mid-Pleistocene temperature record from Arctic Lake El'gygytgyn: a 50 kyr super interglacial from MIS 33 to MIS 31? Earth Planet Sci. Lett. 436, 56–63.

DeConto, R.M., Pollard, D., Kowalewski, D., 2012. Modeling antarctic ice sheet and climate variations during marine isotope stage 31. Global Planet. Change 88–89, 45–52.

Demarchi, B., Collins, M., 2014. Amino acid racemization dating. In: Rink, W.J., Thompson, J. (Eds.), Encyclopedia of Scientific Dating Methods. Springer Netherlands, Dordrecht, pp. 1–22.

Deniel, C., Pin, C., 2001. Single-stage method for the simultaneous isolation of lead and strontium from silicate samples for isotopic measurements. Anal. Chim. Acta 426, 95–103.

DePaolo, D.J., 1986. Detailed record of the Neogene Sr isotopic evolution of seawater from DSDP Site 590B. Geology 14, 103–106.

DePaolo, D.J., Ingram, B.L., 1985. High-resolution stratigraphy with strontium isotopes. Science 227, 938–941.

Dooley, J.H., 2006. In: Kogel, J.E., Trivedi, N.C., Barker, J.M., Krukowski, S.T. (Eds.), Industrial Minerals & Rocks: Commodities, Markets, and Uses. SME.

Eidvin, T., Ottesen, D., Dybkjær, K., Rasmussen, E.S., Riis, F., 2020. The use of Sr isotope stratigraphy to date the Pleistocene sediments of the Norwegian continental shelf – a review. Norw. J. Geol. 100, 202013.

Eidvin, T., Riis, F., Rasmussen, E., Rundberg, Y., 2013. Investigation of Oligocene to lower Pliocene deposits in the nordic offshore area and onshore Denmark. NPD Bull. 10, 62.

Eidvin, T., Riis, F., Rundberg, Y., 1999. Upper cainozoic stratigraphy in the central North sea (ekofisk and sleipner fields). Nor. Geol. Tidsskr. 79, 97–127.

Eidvin, T., Rundberg, Y., 2001. Late Cainozoic stratigraphy of the Tampen area (Snorre and Visund fields) in the northern North Sea, with emphasis on the chronology of early Neogene sands. Nor. Geol. Tidsskr. 81, 119–160.

Eidvin, T., Rundberg, Y., 2007. Post-Eocene strata of the southern Viking Graben, northern North Sea; integrated biostratigraphic, strontium isotopic and lithostratigraphic study. Norwegian J. Geol./Norsk Geologisk Foren. 87.

El Meknassi, S., Dera, G., Cardone, T., De Rafélis, M., Brahmi, C., Chavagnac, V., 2018. Sr isotope ratios of modern carbonate shells: good and bad news for chemostratigraphy. Geology 46, 1003–1006.

Elderfield, H., Ferretti, P., Greaves, M., Crowhurst, S., McCave, I.N., Hodell, D., Piotrowski, A.M., 2012. Evolution of ocean temperature and ice volume through the mid-pleistocene climate transition. Science 337, 704–709.

Evans, J.A., Montgomery, J., Wildman, G., Boulton, N., 2010. Spatial variations in biosphere 87Sr/86Sr in Britain. J. Geol. Soc. 167, 1–4.

Evans, T.R., Coleman, N.C., 1974. North Sea geothermal gradients. Nature 247, 28–30.

Feyling-Hanssen, R.W., 1964. Foraminifera in late quaternary deposits from the oslofjord area. Norges Geologiske Undersøkelser 225, 383pp.

Haflidason, H., Sejrup, H.P., Klitgaard, D., Johnsen, S., 1995. Coupled response of the late glacial climatic shifts of NW-Europe reflected in Greenland ice cores: evidence from the northern North Sea. Geology 23, 1059–1062.

Harper, M.L., 1971. Approximate geothermal gradients in the north sea basin. Nature 230, 235–236.

Head, M.J., Riding, J.B., Eidvin, T., Chadwick, R.A., 2004. Palynological and foraminiferal biostratigraphy of (upper Pliocene) Nordland group mudstones at sleipner, northern North sea. Mar. Petrol. Geol. 21, 277–297.

Hess, J., Bender, M.L., Schilling, J.-G., 1986. Evolution of the ratio of strontium-87 to strontium-86 in seawater from Cretaceous to present. Science 231, 979–984.

Hjelstuen, B.O., Sejrup, H.P., 2020. Latitudinal variability in the Quaternary development of the Eurasian ice sheets—evidence from the marine domain. Geology 49, 346–351.

Holmes, R., 1997. Quaternary stratigraphy: the offshore record. In: Gordon, J.E. (Ed.), Reflections on the Ice Age in Scotland: an Update on Quaternary Studies. The Scottish Association of Geography Teachers and Scottish Natural Heritage, Glasgow, pp. 72–94.

Howarth, R.J., McArthur, J.M., 1997. Statistics for strontium isotope stratigraphy: a robust LOWESS fit to the marine Sr-isotope curve for 0 to 206 Ma, with look-up table for derivation of numeric age. J. Geol. 105, 441–456.

Jouzel, J., Masson-Delmotte, V., Cattani, O., Dreyfus, G., Falourd, S., Hoffmann, G., Minster, B., Nouet, J., Barnola, J.M., Chappellaz, J., Fischer, H., Gallet, J.C., Johnsen, S., Leuenberger, M., Loulergue, L., Luethi, D., Oerter, H., Parrenin, F., Raisbeck, G., Raynaud, D., Schilt, A., Schwander, J., Selmo, E., Souchez, R., Spahni, R., Stauffer, B., Steffensen, J.P., Stenni, B., Stocker, T.F., Tison, J.L., Werner, M., Wolff, E.W., 2007. Orbital and millennial antarctic climate variability over the past 800,000 years. Science 317, 793–796.

Kaufman, D., 2014. Amino acid racemization, marine sediments. In: Rink, W.J., Thompson, J. (Eds.), Encyclopedia of Scientific Dating Methods. Springer Netherlands, Dordrecht, pp. 1–4.
Kaufman, D., Carter, L.D., Miller, G.H., Farmer, G.L., Budd, D.A., 1993. Strontium isotopic composition of Pliocene and Pleistocene molluscs from emerged marine deposits, North American Arctic. Can. J. Earth Sci. 30, 519–534.
Kaufman, D.S., 2000. Amino acid racemization in ostracodes. In: Goodfriend, G., Collin, M., Fogel, M., Macko, S., Wehmiller, J. (Eds.), Perspectives in Amino Acid and Protein Geochemistry. Oxford University Press, New York, pp. 145–160.
Kaufman, D.S., Cooper, K., Behl, R., Billups, K., Bright, J., Gardner, K., Hearty, P., Jakobsson, M., Mendes, I., O'Leary, M., Polyak, L., Rasmussen, T., Rosa, F., Schmidt, M., 2013. Amino acid racemization in mono-specific foraminifera from Quaternary deep-sea sediments. Quat. Geochronol. 16, 50–61.
Kaufman, D.S., Manley, W.F., 1998. A new procedure for determining dl amino acid ratios in fossils using reverse phase liquid chromatography. Quat. Sci. Rev. 17, 987–1000.
Kaufman, D.S., Polyak, L., Adler, R., Channell, J.E.T., Xuan, C., 2008. Dating late Quaternary planktonic foraminifer Neogloboquadrina pachyderma from the Arctic Ocean using amino acid racemization. Paleoceanography 23.
King, E.L., 1991. History of Quaternary Sedimentation in Borehole 77/2, Witch Ground Basin, North Sea, Geologisk Institutt. Universitetet i Bergen, Bergen, p. 131.
Knudsen, K., Asbjörnsdóttir, L., 1991. Plio-pleistocene foraminiferal stratigraphy and correlation in the central North sea. Mar. Geol. 101, 113–124.
Knudsen, K.L., Sejrup, H.P., 1988. Amino acid geochronology of selected interglacial sites in the North Sea area. Boreas 17, 347–354.
Knudsen, K.L., Sejrup, H.P., 1993. Pleistocene stratigraphy in the devils hole area, central North-sea - foraminiferal and amino-acid evidence. J. Quat. Sci. 8, 1–14.
Kosnik, M.A., Kaufman, D.S., 2008. Identifying outliers and assessing the accuracy of amino acid racemization measurements for geochronology: II. Data screening. Quat. Geochronol. 3, 328–341.
Kuznetsov, A., Semikhatov, M., Gorokhov, I., 2012. The Sr isotope composition of the world ocean, marginal and inland seas: implications for the Sr isotope stratigraphy. Stratigr. Geol. Correl. 20, 501–515.
Lamb, R.M., Harding, R., Huuse, M., Stewart, M., Brocklehurst, S.H., 2018. The early Quaternary North sea basin. J. Geol. Soc. 175, 275–290.
Lee, J.R., Rose, J., Hamblin, R.J., Moorlock, B.S., Riding, J.B., Phillips, E., Barendregt, R. W., Candy, I., 2011. The glacial history of the British isles during the early and middle Pleistocene: implications for the long-term development of the British ice sheet. In: Ehlers, J., Gibbard, P.L., Hughes, P.D. (Eds.), Quaternary Glaciations–Extent and Chronology, A Closer Look. Developments in Quaternary Science. Elsevier, Amsterdam, pp. 59–74.
Lonergan, L., Maidment, S.C.R., Collier, J.S., 2006. Pleistocene subglacial tunnel valleys in the central North Sea basin: 3-D morphology and evolution. J. Quat. Sci. 21, 891–903.
Løseth, H., Dowdeswell, J.A., Batchelor, C.L., Ottesen, D., 2020. 3D sedimentary architecture showing the inception of an Ice Age. Nat. Commun. 11, 2975.
McArthur, J.M., Howarth, R.J., Bailey, T.R., 2001. Strontium isotope stratigraphy: LOWESS version 3: best fit to the marine Sr-isotope curve for 0-509 Ma and accompanying look-up table for deriving numerical age. J. Geol. 109, 155–170.
Melles, M., Brigham-Grette, J., Minyuk, P.S., Nowaczyk, N.R., Wennrich, V., DeConto, R. M., Anderson, P.M., Andreev, A.A., Coletti, A., Cook, T.L., Haltia-Hovi, E., Kukkonen, M., Lozhkin, A.V., Rosén, P., Tarasov, P., Vogel, H., Wagner, B., 2012. 2.8 million years of arctic climate change from lake el'gygytgyn, NE Russia. Science 337, 315.
Miller, G.H., Brigham-Grette, J., 1989. Amino acid geochronology: resolution and precision in carbonate fossils. Quat. Int. 1, 111–128.
Morrison, F.A., 2015. Obtaining Uncertainty Measures on Parameters of a Polynomial Least Squares Fit with Excel's LINEST. Michigan Technological University, Houghton, MI. Available at: https://pages.mtu.edu/~fmorriso/cm3215/UncertaintyPolynomialLeastSquaresFit_LINEST_v1.pdf.
Ottesen, D., Batchelor, C.L., Dowdeswell, J.A., Loseth, H., 2018. Morphology and pattern of quaternary sedimentation in the north sea basin (52-62 degrees N). Mar. Petrol. Geol. 98, 836–859.
Ottesen, D., Dowdeswell, J.A., Bugge, T., 2014. Morphology, sedimentary infill and depositional environments of the early Quaternary North sea basin (56 degrees-62 degrees N). Mar. Petrol. Geol. 56, 123–146.
Overeem, I., Weltje, G.J., Bishop-Kay, C., Kroonenberg, S.B., 2001. The late cenozoic Eridanos delta system in the southern North sea basin: a climate signal in sediment supply? Basin Res. 13, 293–312.
Piasecki, S., Gregersen, U., Johannessen, P.N., 2002. Lower Pliocene dinoflagellate cysts from cored Utsira Formation in the viking graben, northern North sea. Mar. Petrol. Geol. 19, 55–67.
Prokopenko, A.A., Williams, D.F., Kuzmin, M., Karabanov, E.B., Khursevich, G.K., Peck, J.A., 2002. Muted climate variations in continental Siberia during the mid-Pleistocene epoch. Nature 418, 65–68.
Rea, B.R., Newton, A.M.W., Lamb, R.M., Harding, R., Bigg, G.R., Rose, P., Spagnolo, M., Huuse, M., Cater, J.M.L., Archer, S., Buckley, F., Halliyeva, M., Huuse, J., Cornwell, D.G., Brocklehurst, S.H., Howell, J.A., 2018. Extensive marine-terminating ice sheets in Europe from 2.5 million years ago. Sci. Adv. 4, eaar8327.
Reinardy, B.T.I., Hjelstuen, B.O., Sejrup, H.P., Augedal, H., Jorstad, A., 2017. Late Pliocene-Pleistocene environments and glacial history of the northern North Sea. Quat. Sci. Rev. 158, 107–126.
Reinardy, B.T.I., Sejrup, H.P., Hjelstuen, B.O., King, E., Augedal, H., 2018. A Quaternary aminostratigraphy constraining chronology of depositional environments in the North Sea Basin. Mar. Geol. 402, 139–152.
Rise, L., Olesen, O., Rokoengen, K., Ottesen, D., Riis, F., 2004. Mid-Pleistocene ice drainage pattern in the Norwegian Channel imaged by 3D seismic. Quat. Sci. Rev. 23, 2323–2335.
Rohling, E.J., Foster, G.L., Grant, K.M., Marino, G., Roberts, A.P., Tamisiea, M.E., Williams, F., 2014. Sea-level and deep-sea-temperature variability over the past 5.3 million years. Nature 508, 477–482.
Scherer, R.P., Bohaty, S.M., Dunbar, R.B., Esper, O., Flores, J.A., Gersonde, R., Harwood, D.M., Roberts, A.P., Taviani, M., 2008. Antarctic records of precession-paced insolation-driven warming during early Pleistocene Marine Isotope Stage 31. Geophys. Res. Lett. 35.
Sejrup, H.-P., Miller, G.H., Brigham-Grette, J., Løvlie, R., Hopkins, D., 1984. Amino acid epimerization implies rapid sedimentation rates in arctic ocean cores. Nature 310, 772–775.
Sejrup, H.P., Haflidason, H., Aarseth, I., King, E., Forsberg, C.F., Long, D., Rokoengen, K., 1994. Late weichselian glaciation history of the northern North-sea. Boreas 23, 1–13.
Sejrup, H.P., Haugen, J.-E., 1992. Foraminiferal amino acid stratigraphy of the Nordic Seas: geological data and pyrolysis experiments. Deep Sea Res. 39, 603–s623.
Sejrup, H.P., Hjelstuen, B.O., Nygård, A., Haflidason, H., Mardal, I., 2015. Late Devensian ice-marginal features in the central North Sea - processes and chronology. Boreas 44, 1–13.
Sejrup, H.P., Knudsen, K.L., 1993. Paleoenvironments and correlations of interglacial sediments in the north-sea. Boreas 22, 223–235.
Sejrup, H.P., Knudsen, K.L., 1999. Geochronology and palaeoenvironment of marine Quaternary deposits in Denmark: new evidence from northern Jutland. Geol. Mag. 136, 561–578.
Sejrup, H.P., Landvik, J.Y., Larsen, E., Janocko, J., Eiriksson, J., King, E., 1998. The Jaeren area, a border zone of the Norwegian channel ice stream. Quat. Sci. Rev. 17, 801–812.
Sejrup, H.P., Larsen, E., Haflidason, H., Berstad, I.M., Hjelstuen, B.O., Jonsdottir, H.E., King, E.L., Landvik, J., Longva, O., Nygard, A., Ottesen, D., Raunholm, S., Rise, L., Stalsberg, K., 2003. Configuration, history and impact of the Norwegian channel ice stream. Boreas 32, 18–36.
Sejrup, H.P., Larsen, E., Landvik, J., King, E.L., Haflidason, H., Nesje, A., 2000. Quaternary glaciations in southern Fennoscandia: evidence from southwestern Norway and the northern North Sea region. Quat. Sci. Rev. 19, 667–685.
Sejrup, H.P., Nagy, J., Brighamgrette, J., 1989. Foraminiferal stratigraphy and amino-acid geochronology of quaternary sediments in the Norwegian channel, northern North-sea. Nor. Geol. Tidsskr. 69, 111–124.
Sejrup, H.P., Aarseth, I., Ellingsen, K.L., Løvlie, R., Reither, E., Bent, A., Brigham-Grette, J., Jansen, E., Larsen, E., Stoker, M., 1987. Quaternary stratigraphy of the Fladen area, central North Sea: a multidisciplinary study. J. Quat. Sci. 2, 35–58.
Sejrup, H.P., Aarseth, I., Haflidason, H., 1991. The quaternary succession in the northern North-sea. Mar. Geol. 101, 103–111.
Sejrup, H.P., Aarseth, I., Haflidason, H., Lovlie, R., Bratten, A., Tjostheim, G., Forsberg, C.F., Ellingsen, K.L., 1995. Quaternary of the Norwegian channel - glaciation history and paleoceanography. Nor. Geol. Tidsskr. 75, 65–87.
Stoker, M.S., Skinner, A.C., Fyfe, J.A., Long, D., 1983. Palaeomagnetic evidence for early Pleistocene in the central and northern North Sea. Nature 304, 332–334.
Voelker, A.H.L., Rodrigues, T., Billups, K., Oppo, D., McManus, J., Stein, R., Hefter, J., Grimalt, J.O., 2010. Variations in mid-latitude North Atlantic surface water properties during the mid-Brunhes (MIS 9–14) and their implications for the thermohaline circulation. Clim. Past 6, 531–552.
Wehmiller, J.F., Harris, W.B., Boutin, B.S., Farrell, K.M., 2012. Calibration of amino acid racemization (AAR) kinetics in United States Mid-Atlantic Coastal Plain Quaternary mollusks using 87Sr/86Sr analyses: evaluation of kinetic models and estimation of regional late Pleistocene temperature history. Quat. Geochronol. 7, 21–36.